Supplementary Information

A Versatile DNA Origami Based Plasmonic Nanoantenna for Label-Free Single-Molecule Surface-Enhanced Raman Spectroscopy (SERS)

Kosti Tapio[1], Amr Mostafa[1], Yuya Kanehira[1], Antonio Suma[2,3], Anushree Dutta[1], Ilko Bald[1*]

[1]*Institute of Chemistry, University of Potsdam, Potsdam, DE-14476 Germany*

[2]*Institute for Computational Molecular Science, Temple University, Philadelphia, PA 19122, Pennsylvania, USA*

[3]*Dipartimento di Fisica, Università di Bari, and Sezione INFN di Bari, 70126 Bari, Italy*

*corresponding author: ilko.bald@uni-potsdam.de

Table of Contents

1. DNA origami fork design

The DNA origami fork design with the nanoparticle capture strands is shown in Figure S1. The DNA origami nanofork is designed such that the scaffold DNA strand is routed through both DNA bridge helices. There are two times 5'-A_{24} and two times 3'-$(AAC)_8$ strands extending from each arm on each side. In addition, there are two times 5'-A_{24} and two times 3'-$(AAC)_8$ extending from the side of the bridge. Each particle capture sequence binds with the coating sequence in a zipper configuration, to ensure a close position of the particles to the bridge. One side of the arms is left open on purpose to enable free diffusion of external molecules into the hot spot if desired.

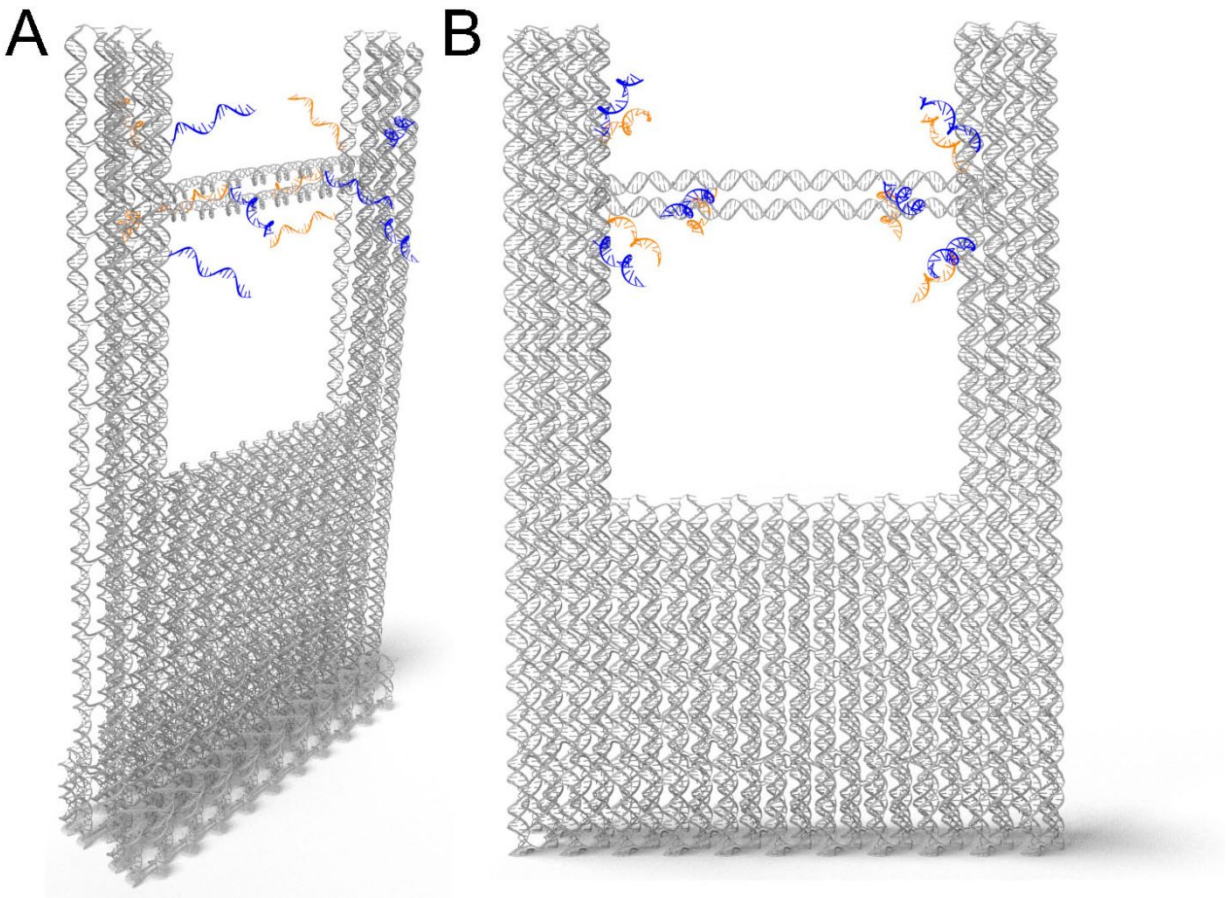

Figure S1. a schematic view of the DNA origami nanofork structures. (A), a side view of the nanofork with two different metal nanoparticle capture strands (blue and orange) protruding from each side of the fork from the arms and the bridge. (B) a side view of the same nanofork.

2. TEM images of Au DONAs

The TEM images of the Au DONAs do not show the actual DNA origami structure although negative staining was used (as in the TEM images of the nanofork structures alone), because the size of the DNA origami is too small and the material contrast too weak compared to the 60 nm Au particles.

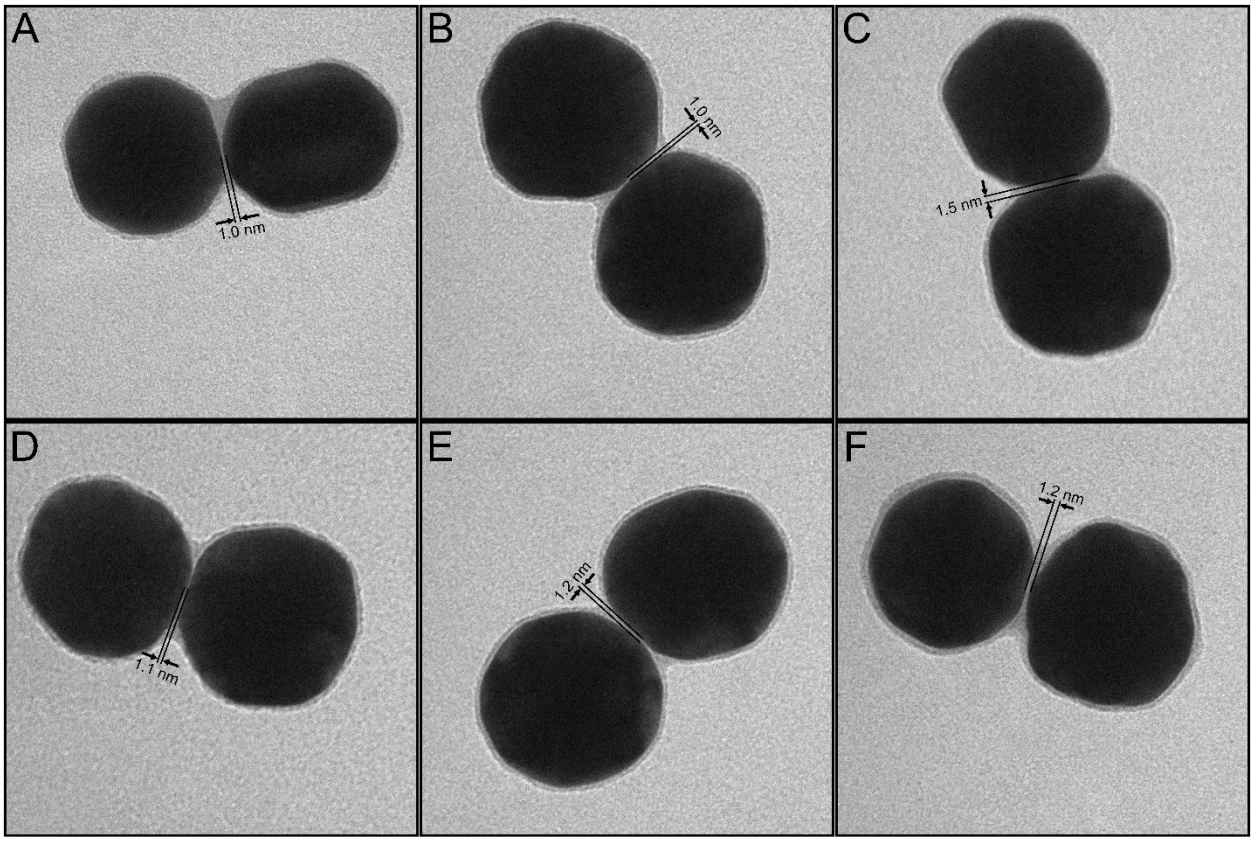

Figure S2. (A)-(F) TEM images of shorter gap size DONA-AuNP dimers. The size of each image is 150 nm x 150 nm.

3. AFM images of Au DONA dimers

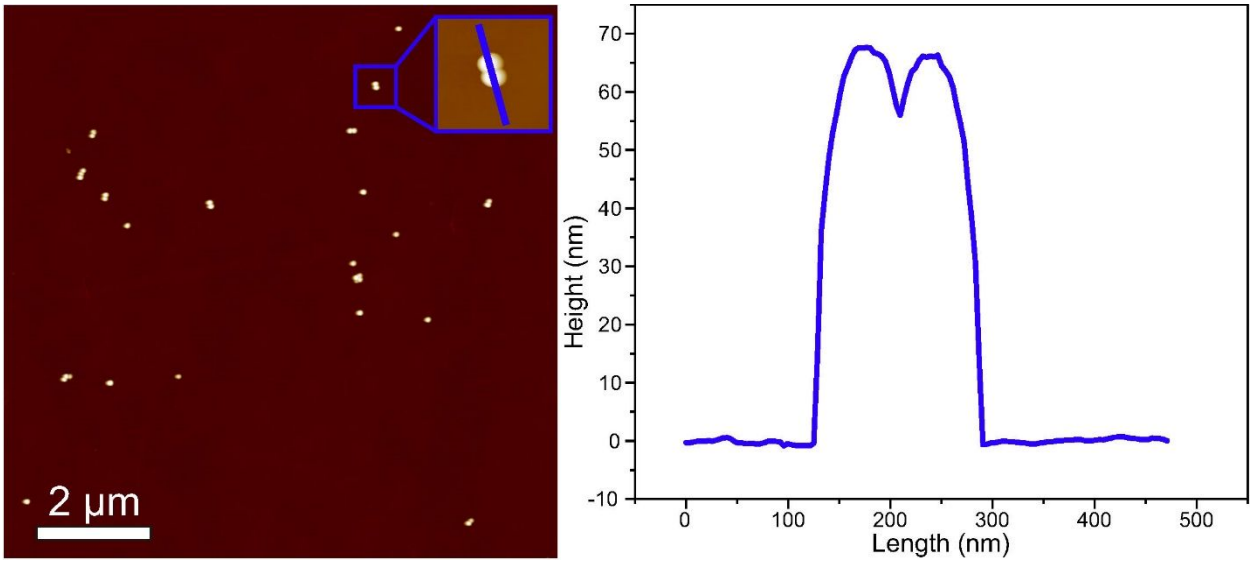

Figure S3. AFM image of Au DONA on a silicon substrate. The height profile of the dimer in the inset is shown on the right.

4. Single NP to DONA dimer ratio calculation

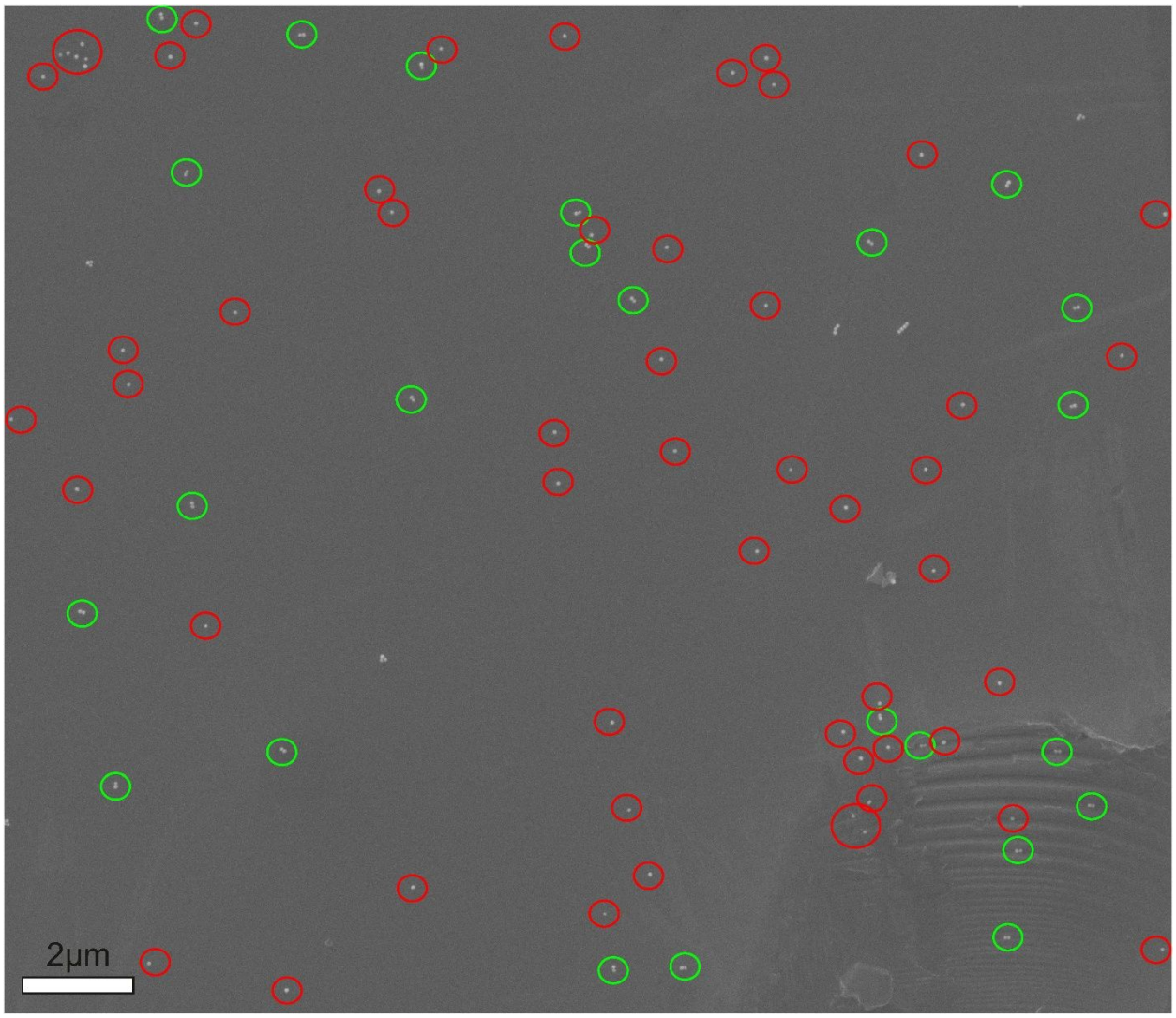

Figure S4. Example SEM image of Au DONA sample used the single NP to DONA dimer ratio calculation. The single NPs and dimers are highlighted by red and green circles, respectively.

5. AFM image of Au DONA monomers

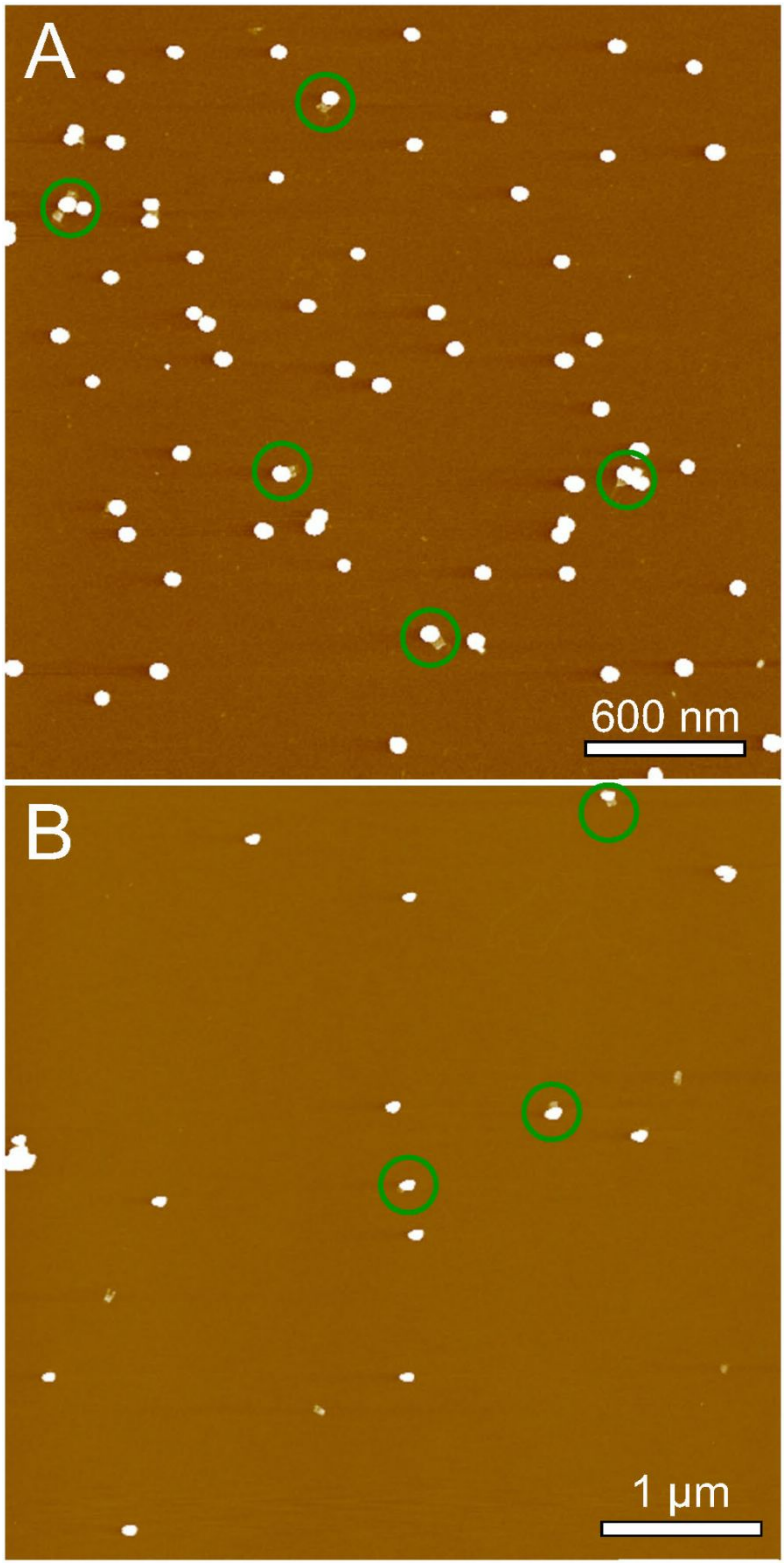

Figure S5. AFM images of 40 nm AuNP monomer DONAs. (A) monomer DONAs with only poly(T) coated particles. (B) monomer DONAs with only $(GTT)_8T_4$ coated particles.

6. AFM images of different DNA origami nanoforks

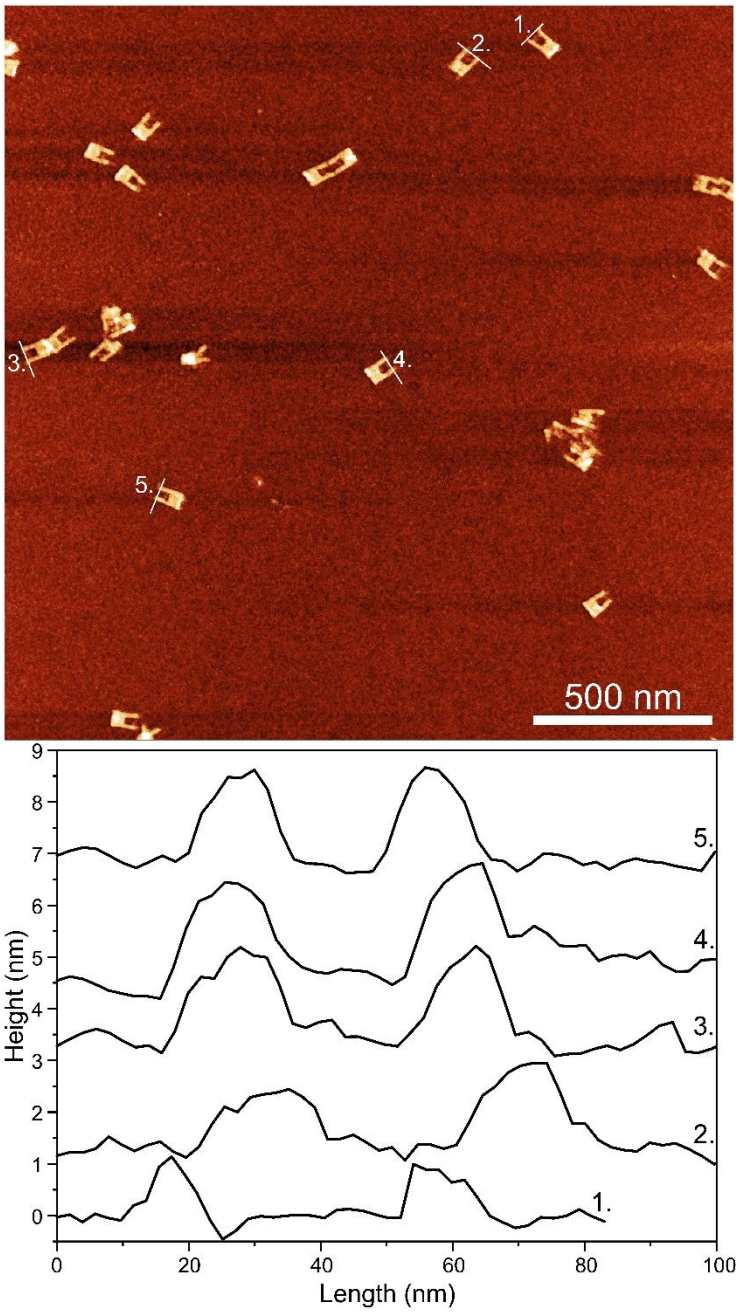

Figure S6. AFM image of the short bridge Forks. The lines and the numbering correspond to the height data.

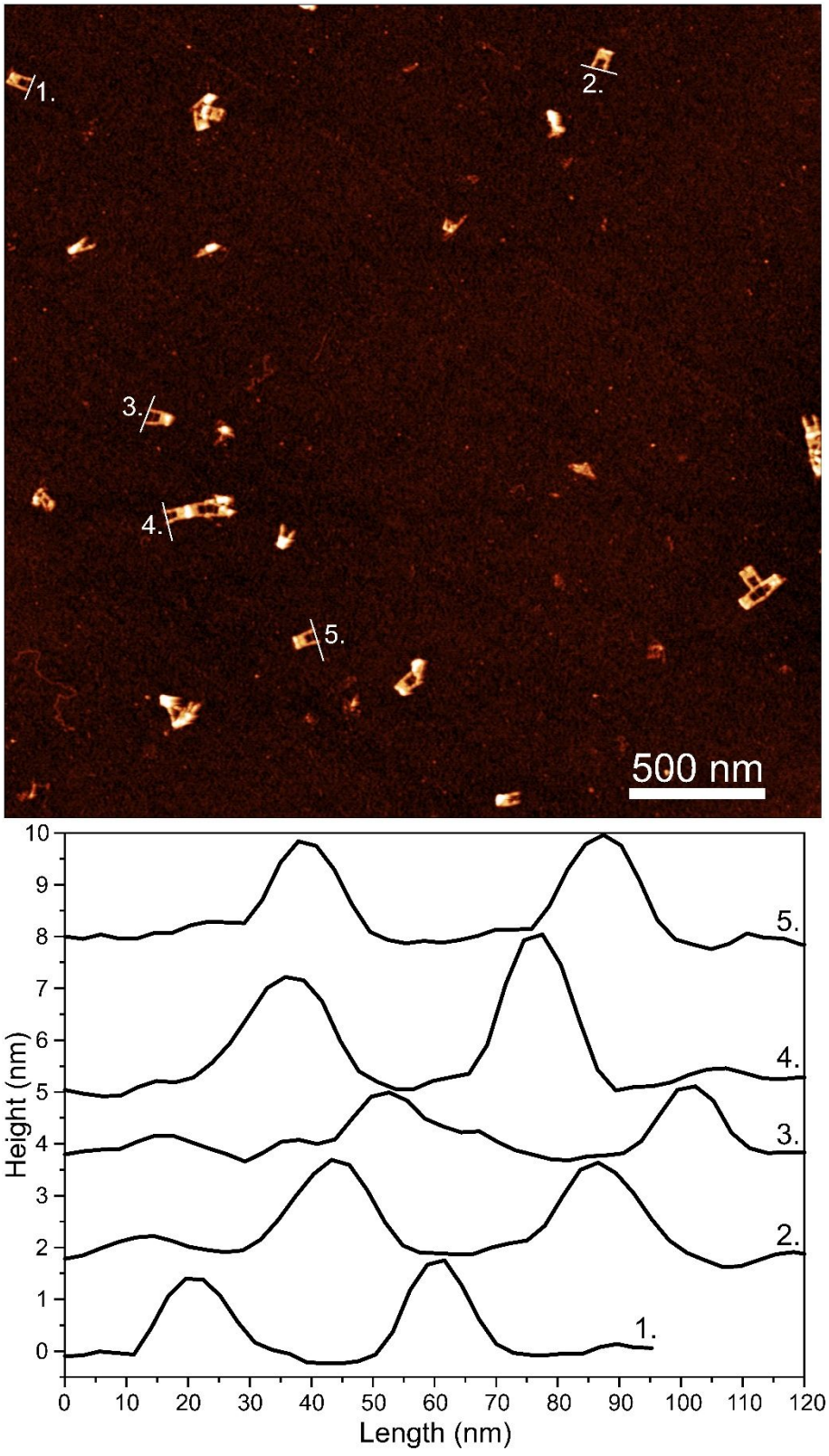

Figure S7. AFM image of the long bridge nanoforks. The lines and the numbering correspond to the height data.

7. The Correlated Raman-SEM maps of dye Ag and Au DONAs

The experimental parameters and the description of the measurements are discussed in the Methods section and the Raman measurement section below. Typically, the SEM images covered a smaller area than the Raman maps, so several SEM maps were stitched together to form an overall SEM map of the corresponding Raman map. The scale bars were used to fix the sizes of the overall SEM and Raman maps to the same size in Corel Draw. Then the maps were superimposed and the positions of the dimers were identified. The small step size was employed in order to achieve good enough overlap between adjacent points in the Raman map. Also, we excluded any dimers from the analysis that had larger aggregates, trimers or tetramers close by, since the assignment of the signal is not clear in these cases.

We observed that the typical TAMRA bands appear at around 1651 cm^{-1} (ν(C=O)/ν(C=C)), 1532 cm^{-1}, 1509 cm^{-1} (both ν(CC)) and 1360 cm^{-1} (δ(COH)/ν(CC)),[1] which is accompanied by contributions from DNA coating strands (*e.g.* the band at 1608 cm^{-1}). For Cy3.5, the characteristic peaks at around 1600 cm^{-1} (ν(C=O)/ν(C=C)), 1450 cm^{-1} and 1285 cm^{-1}. For Cy5, the characteristic bands are at 1592 cm^{-1} (ν(C=O)/ν(C=C)), 1468 cm^{-1} (ν(CC)), 1368 cm^{-1} (δ(COH)/ν(CC)) and 1232 cm^{-1} (ν(CN)).

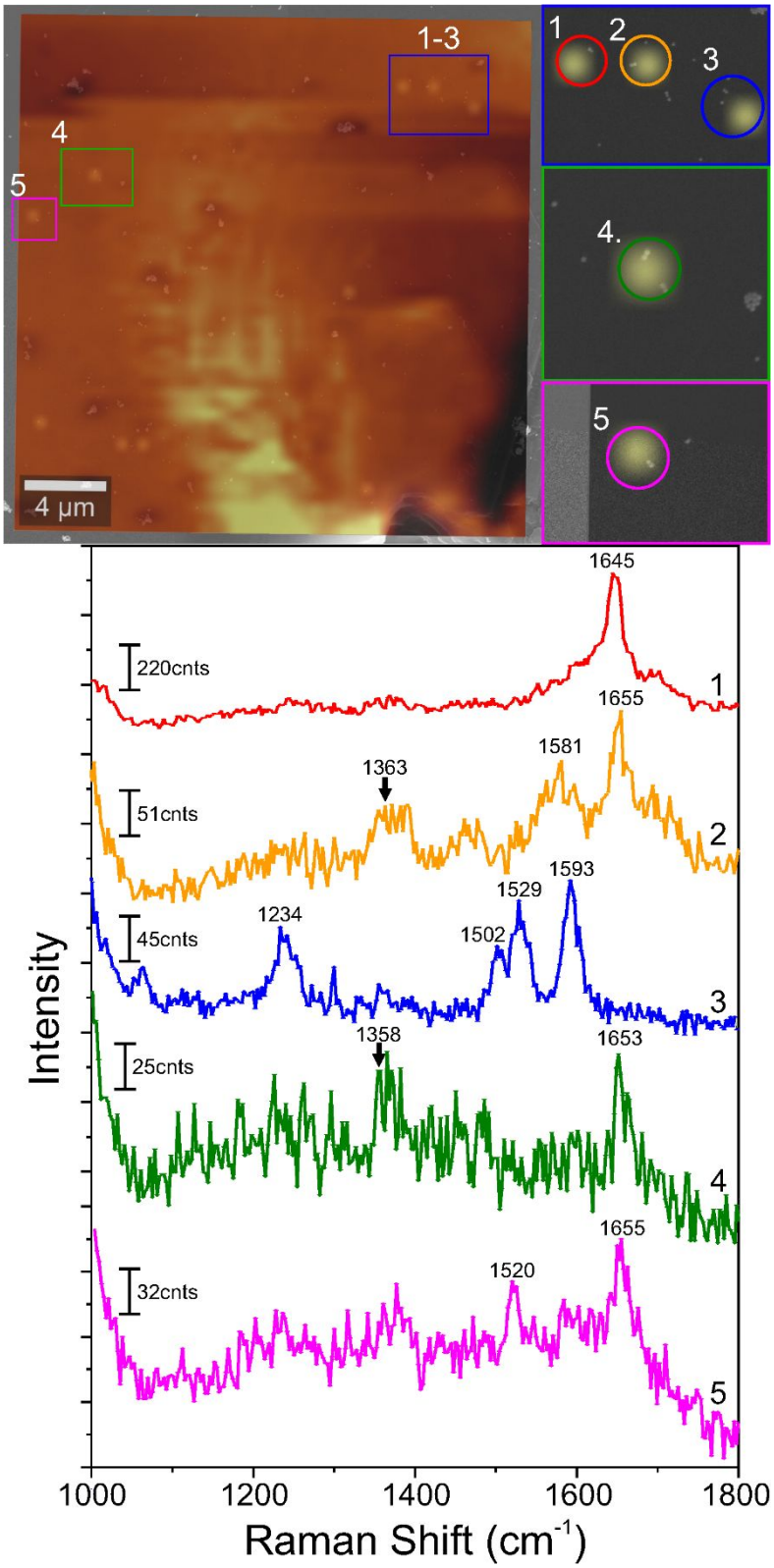

Figure S8. correlated SEM and Raman maps of Tamra modified DONA-AuNP sample. The colors and the number indicate the dimers areas and the corresponding spectra.

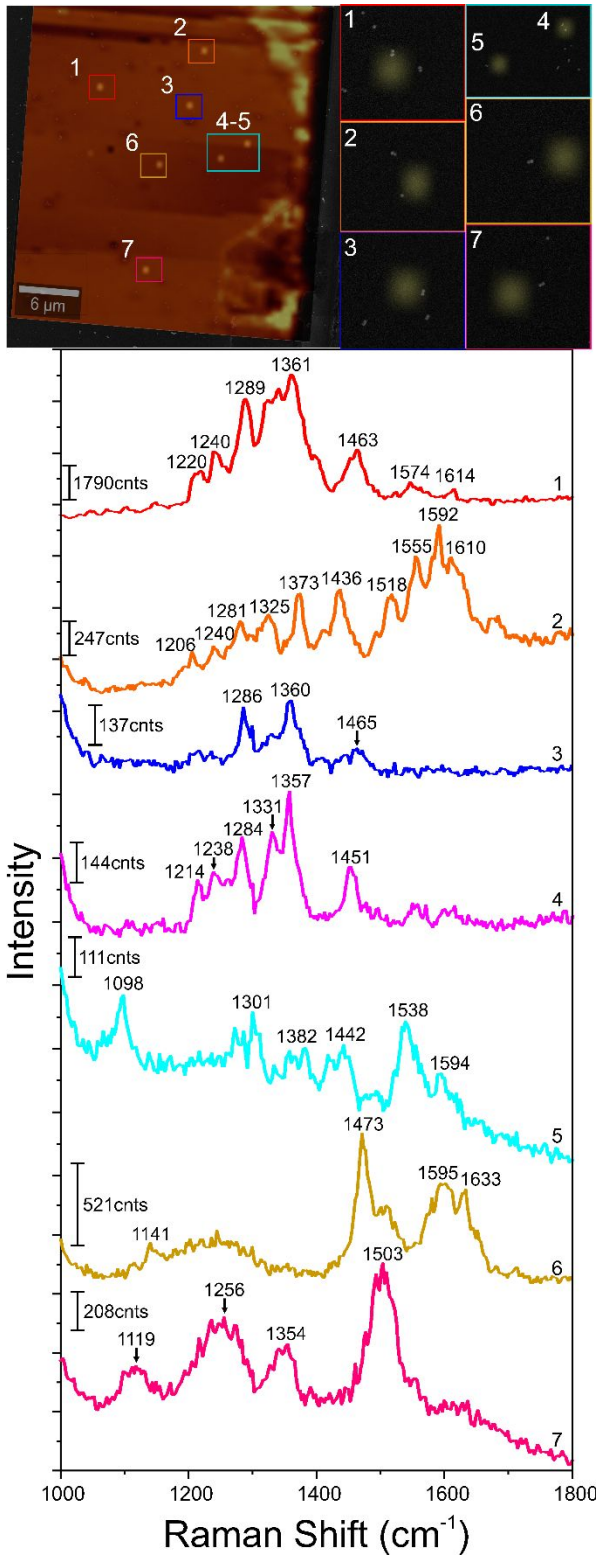

Figure S9. correlated SEM and Raman maps of Cy5 modified DONA-AuNP sample. The colors and the number indicate the dimers areas and the corresponding spectra.

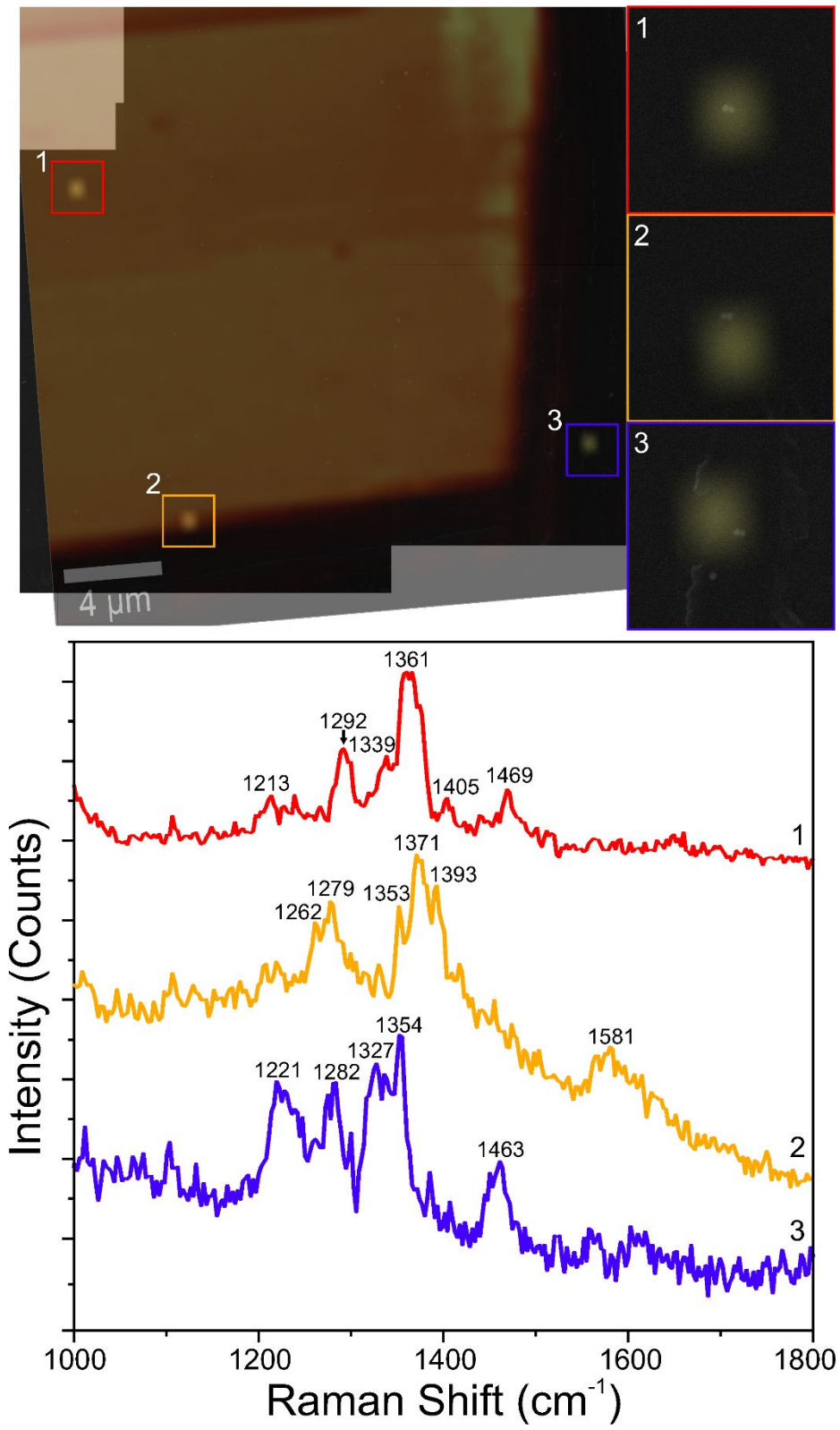

Figure S10. correlated SEM and Raman maps of Cy3.5 modified DONA-AuNP sample. The colors and the number indicate the dimers areas and the corresponding spectra.

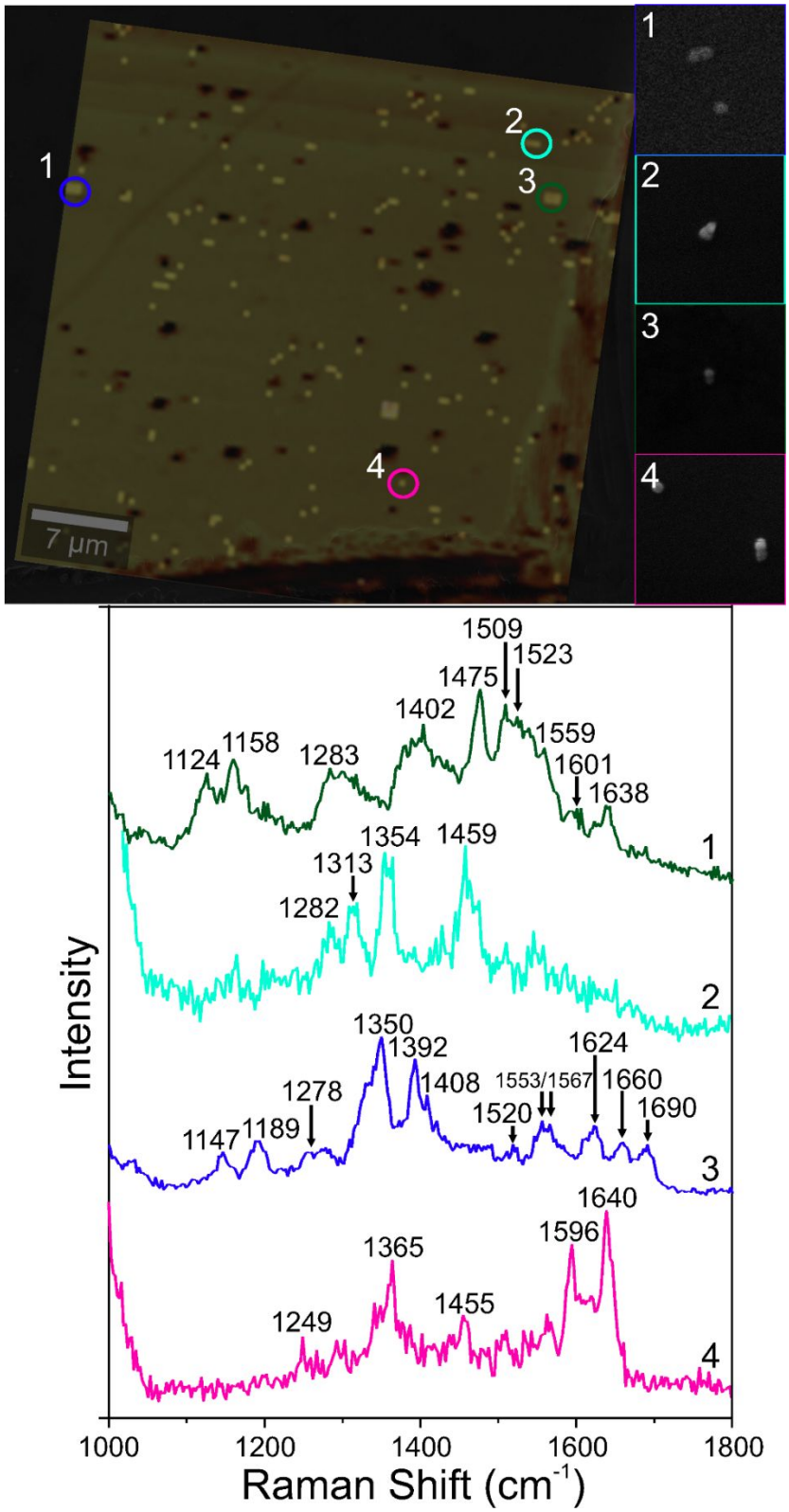

Figure S11. correlated SEM and Raman maps of Cy3.5 modified DONA-AgNP sample. The colors and the number indicate the dimers areas and the corresponding spectra.

8. The Raman reference spectra for the dye and the poly(T)

The dye-nanoparticle reference samples were prepared using the same coating protocol described in the Methods section. Each reference oligo sequence has the form of T_{28} – X – SH, where X is either Tamra, Cy5 or Cy3.5 in the case of dyes or empty for the pure poly(T) DNA reference. The dyes were always positioned close to the particle surface to maximize the plasmonic enhancement of the NP. The dye coated particles were deposited on silicon surface similarly as the DONAs. For gold, the Tamra and the poly(T) references were measured using 10s integration time and 10 accumulations and the power density was 602 W/cm^2 for 633 nm laser. For gold and Cy3.5, the same parameters were 4s, 10 accumulations and 6155 W/cm^2. For gold and Cy5, the parameters were 4 s, 10 accumulations and 4303 W/cm^2 for 633 nm laser. For silver and Tamra or Cy3.5, 1 s and 10 accumulations were used while for poly(T) 4s and 5 accumulations were used. All had a power density of 3070 W/cm^2 for the 532 nm laser. The Figure S12 and Figure S13 show the reference spectra for gold and silver, respectively.

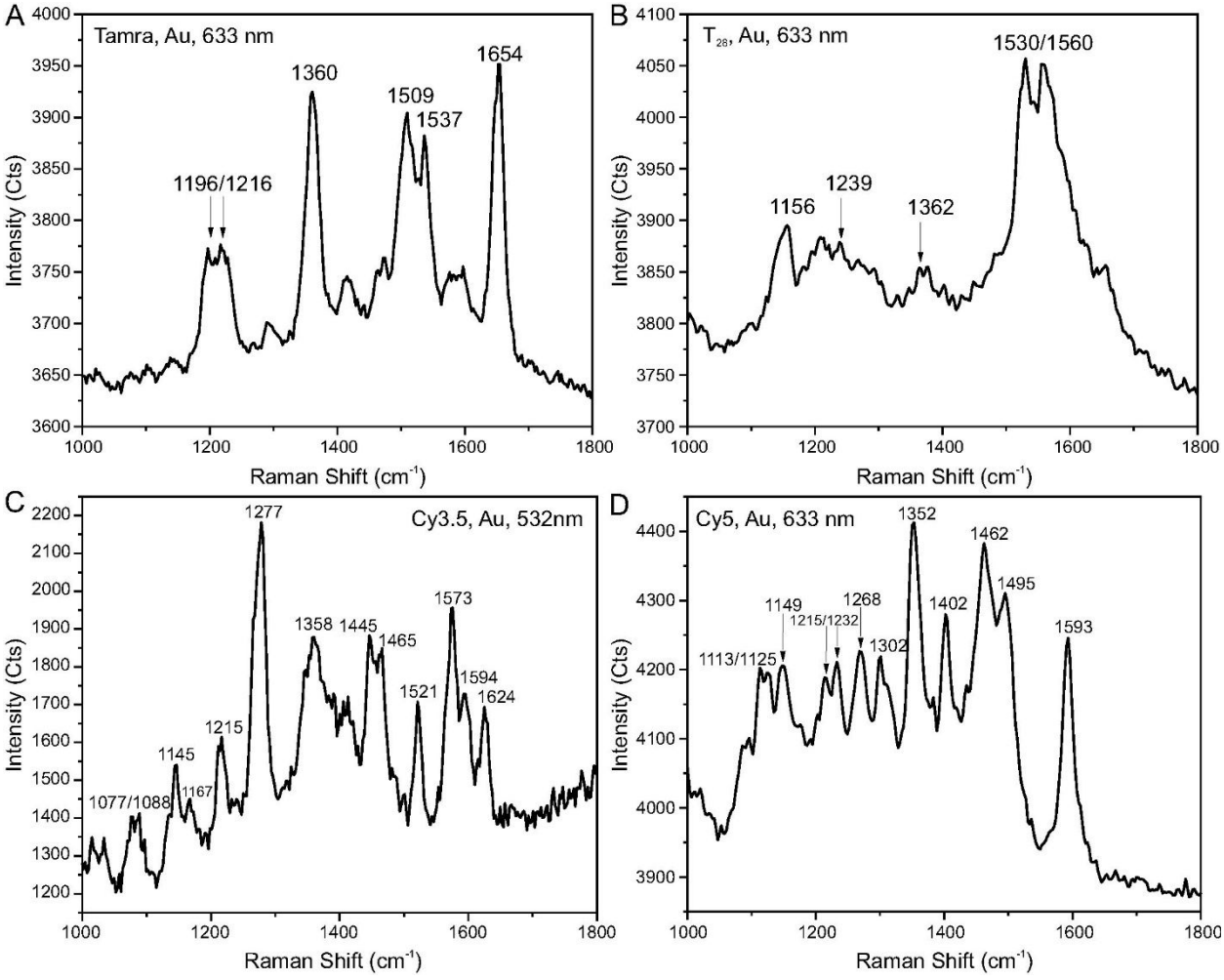

Figure S12. Raman spectra of dye and poly(T) reference samples. (A) Tamra-oligo coated AuNP spectra measured using 633 nm laser. (B) T_{28}-oligo coated AuNP spectra measured using 633 nm laser. (C) Cy3.5-oligo coated AuNP spectra measured using 532 nm laser. (D) Cy5-oligo coated AuNP spectra measured using 633 nm laser.

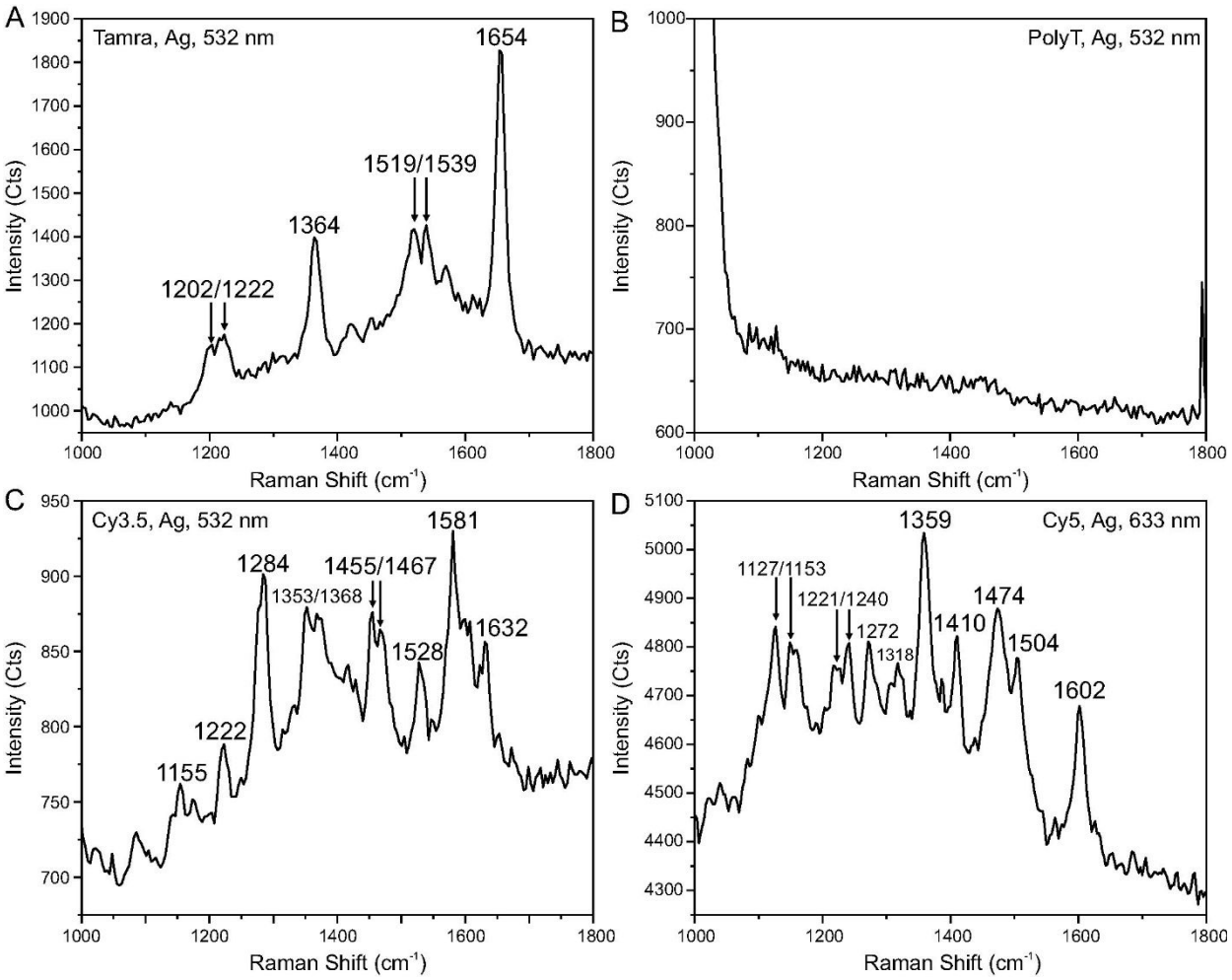

Figure S13. Raman spectra of dye and poly(T) reference samples. (A) Tamra-oligo coated AgNP spectra measured using 532 nm laser. (B) T_{28}-oligo coated AgNP spectra measured using 532 nm laser. (C) Cy3.5-oligo coated AgNP spectra measured using 532 nm laser. (D) Cy5-oligo coated AgNP spectra measured using 633 nm laser.

In DONAs, all dyes were measured using 633 nm laser with 3227 W/cm^2 power density. For Cy3.5 and Cy5, the integration time was 7s and for Tamra 4s. The pure DNA bridge Au DONAs were measured using 5s and 4635 W/cm^2 power density for 532 nm and 7s and 3240 W/cm^2 for 633 nm laser. In Ag DONAs, Tamra and Cy3.5 sample were acquired using 532nm laser with 4605 W/cm^2 power density and 10 and 8 s integration times, respectively. We did not observe any SM SERS signals at 532 nm using Au DONAs, which is in accordance with the FDTD simulations. For the pure DNA bridge case, the integration time was 8 s for both 532 nm and 633 nm laser and the power densities were 3070 and 2152 W/cm^2, respectively. Due to the raster scanning feature, the accumulation was 1.

9. UV-vis absorption spectra of Tamra, Cy5 and Cy3.5 oligos

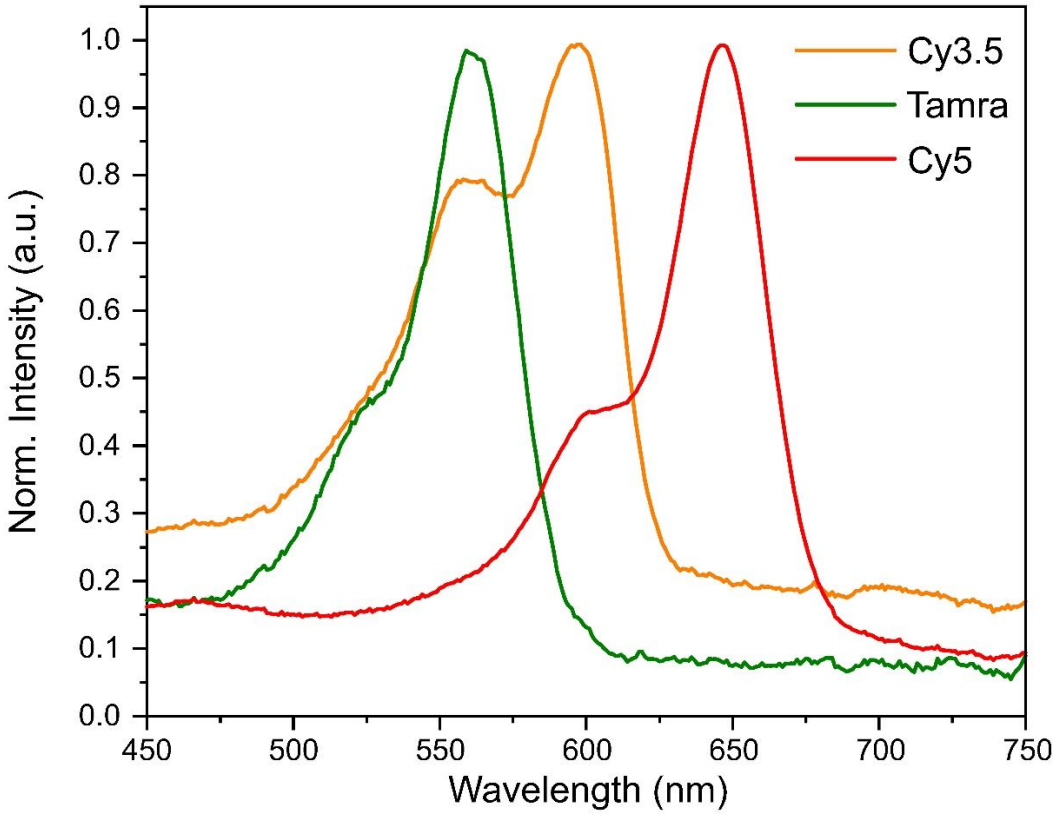

Figure S14. normalized UV-vis absorption spectra of Tamra-, Cy5 and Cy3.5-oligos used in the DONA experiments. The absorption spectrum of TAMRA shows a main absorption band peaking at 561 nm and a shoulder at 530 nm. The main band and the shoulder for Cy3.5 appears at 597 and 560 nm, respectively. Cy5 has the same bands at 646 nm and 606 nm.

10. The average SERS spectra of DNA and dye Au DONAs

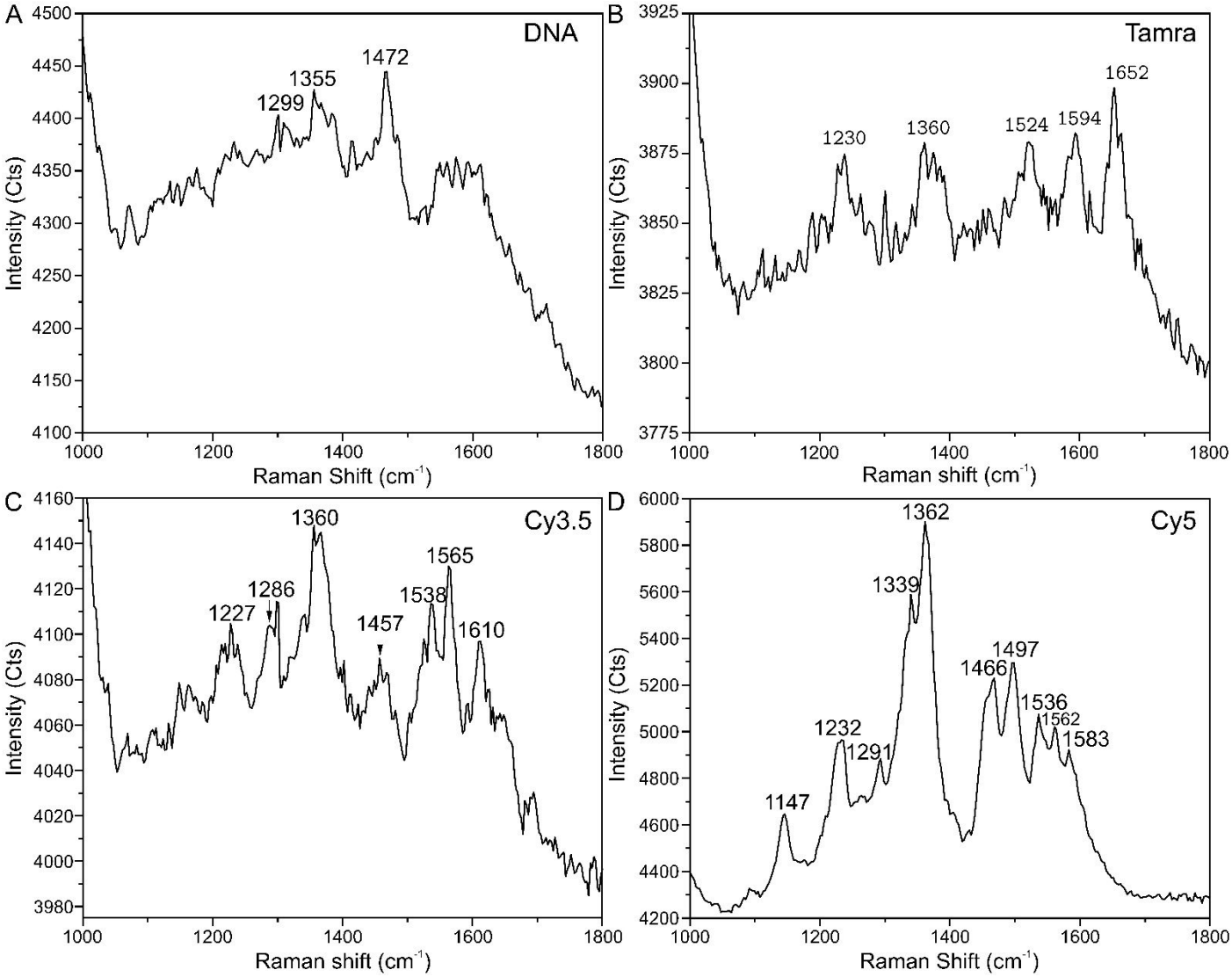

Figure S15. average spectra of multiple, individual-dimer spectra of (A) pure DNA bridge Au DONAs, (B) Tamra Au DONAs, (C) Cy3.5 Au DONAs and (D) Cy5 Au DONAs.

11. The correlated Raman-SEM maps of pure DNA bridge (control) Ag and Au DONAs

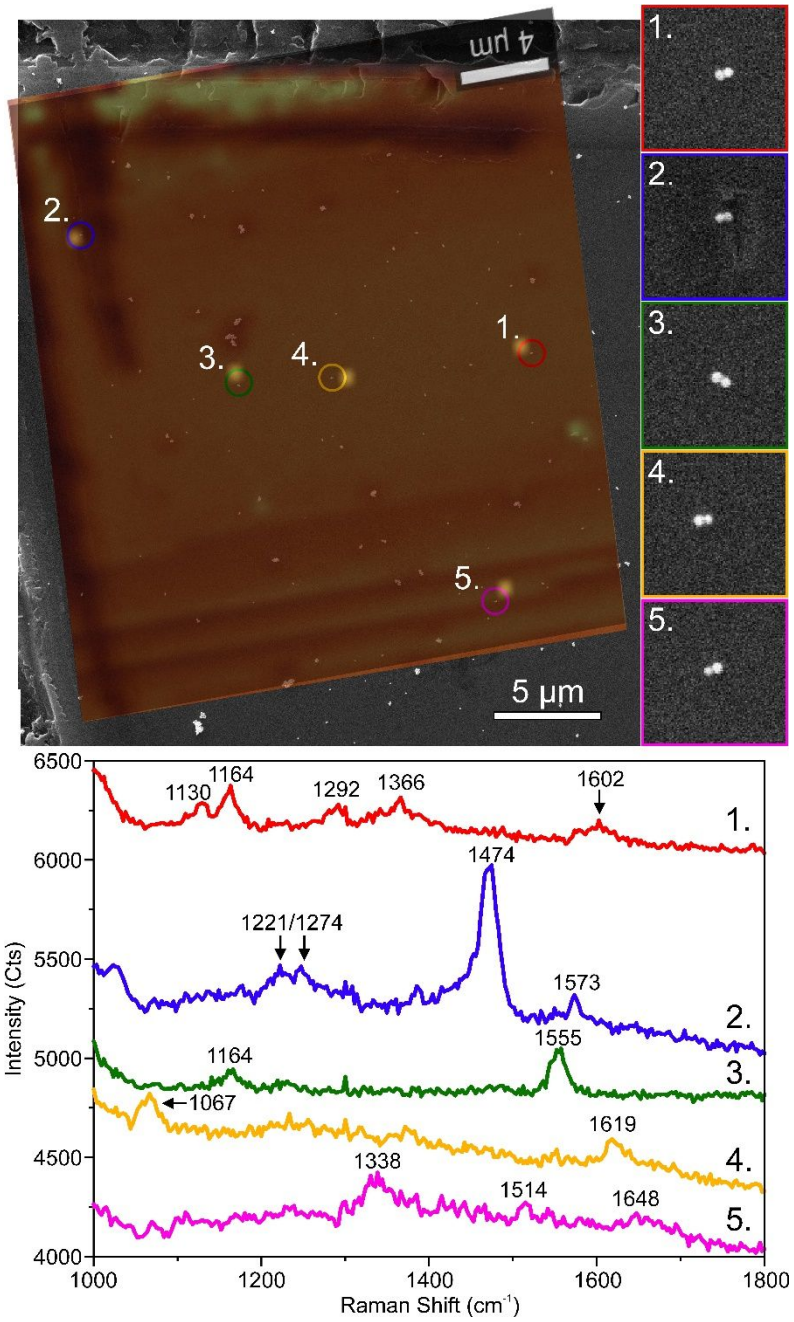

Figure S16. correlated SEM and Raman maps of Au DONA sample, where the bridge contains only DNA. The wavelength of the excitation laser is 633 nm. The colors and the number indicate the dimers areas and the corresponding spectra. The size of the inset images on the right are 1 µm × 1µm.

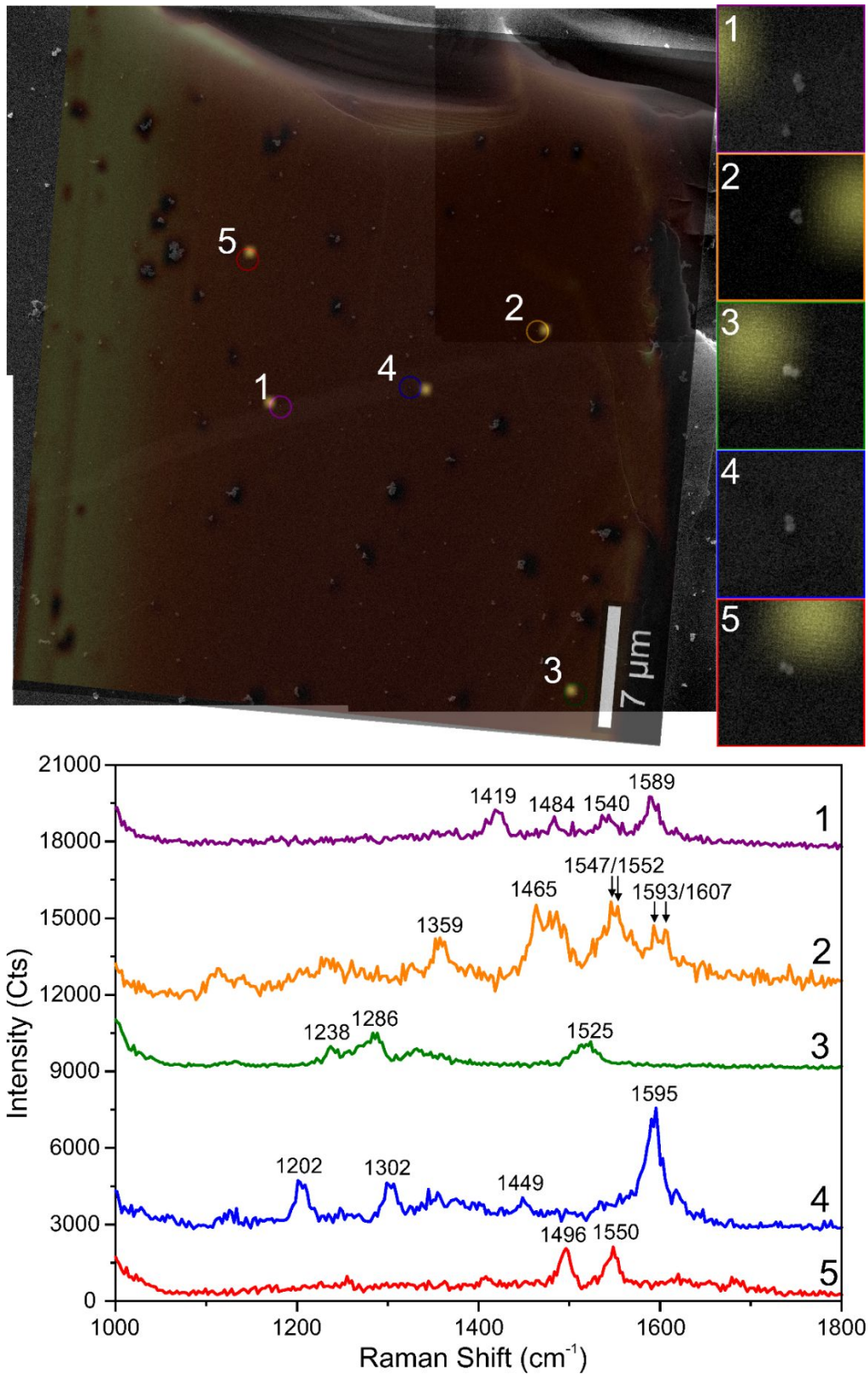

Figure S17. *correlated SEM and Raman maps of Ag DONA sample, where the bridge contains only DNA. The wavelength of the excitation laser is 532 nm. The colors and the numbers indicate the dimer areas and the corresponding spectra. The size of the inset images on the right are 1 µm × 1µm.*

12. Dark field scattering spectra of Au DONAs

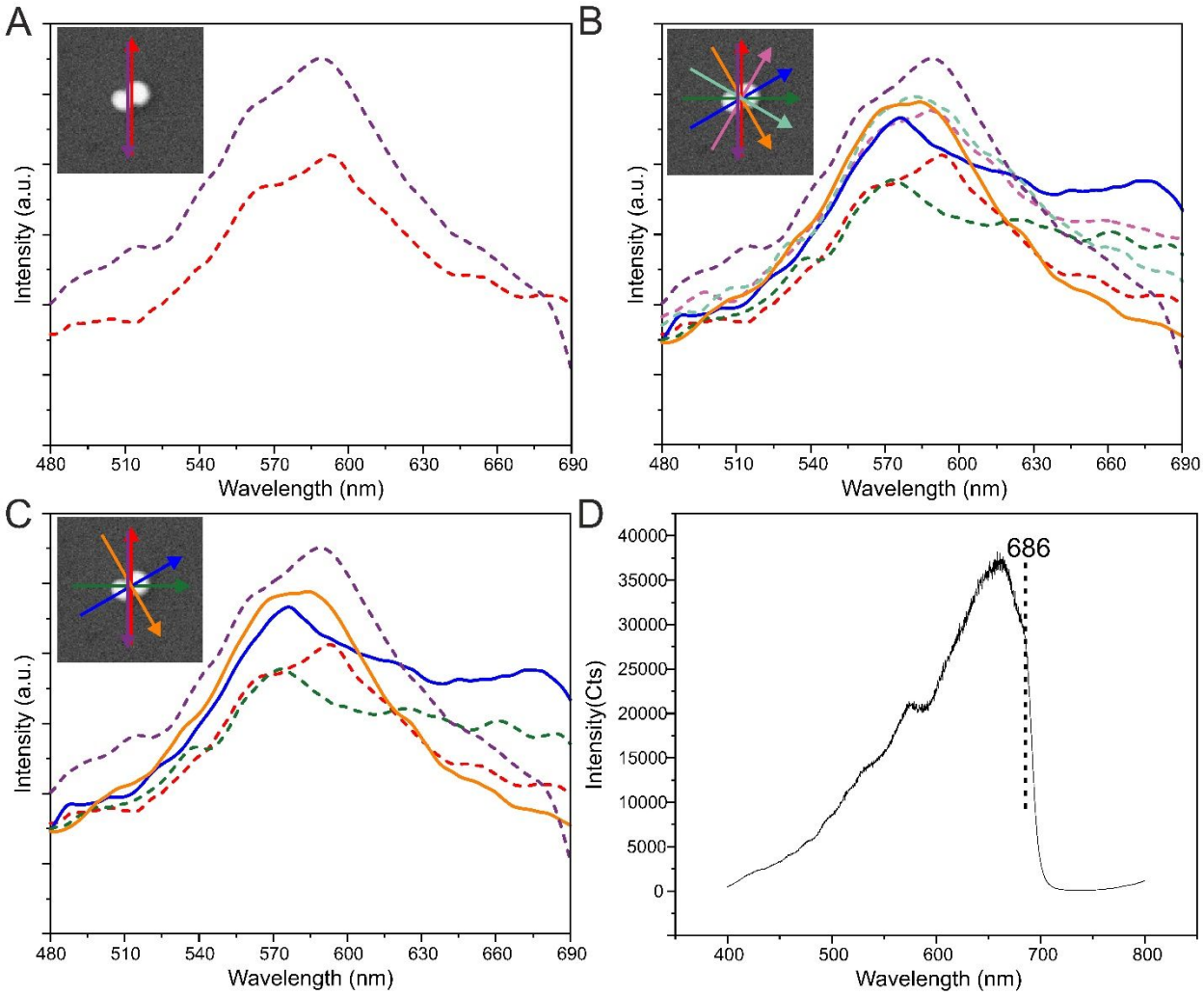

Figure S18. *Polarization dependent dark field (DF) scattering spectra from single dimer. (A) DF scattering spectra corresponding to the directions highlight in the inset. By turning the polarization 180°, the same initial spectral shape can be achieved. Differences in the height of the peaks are most probably due to slightly different focus. (B) DF scattering spectra showing all the measured orientation. (C) DF scattering spectra showing only the selected orientation near the gap axis and the transverse axis. (D) The spectrum of the halogen lamp used in the excitation.*

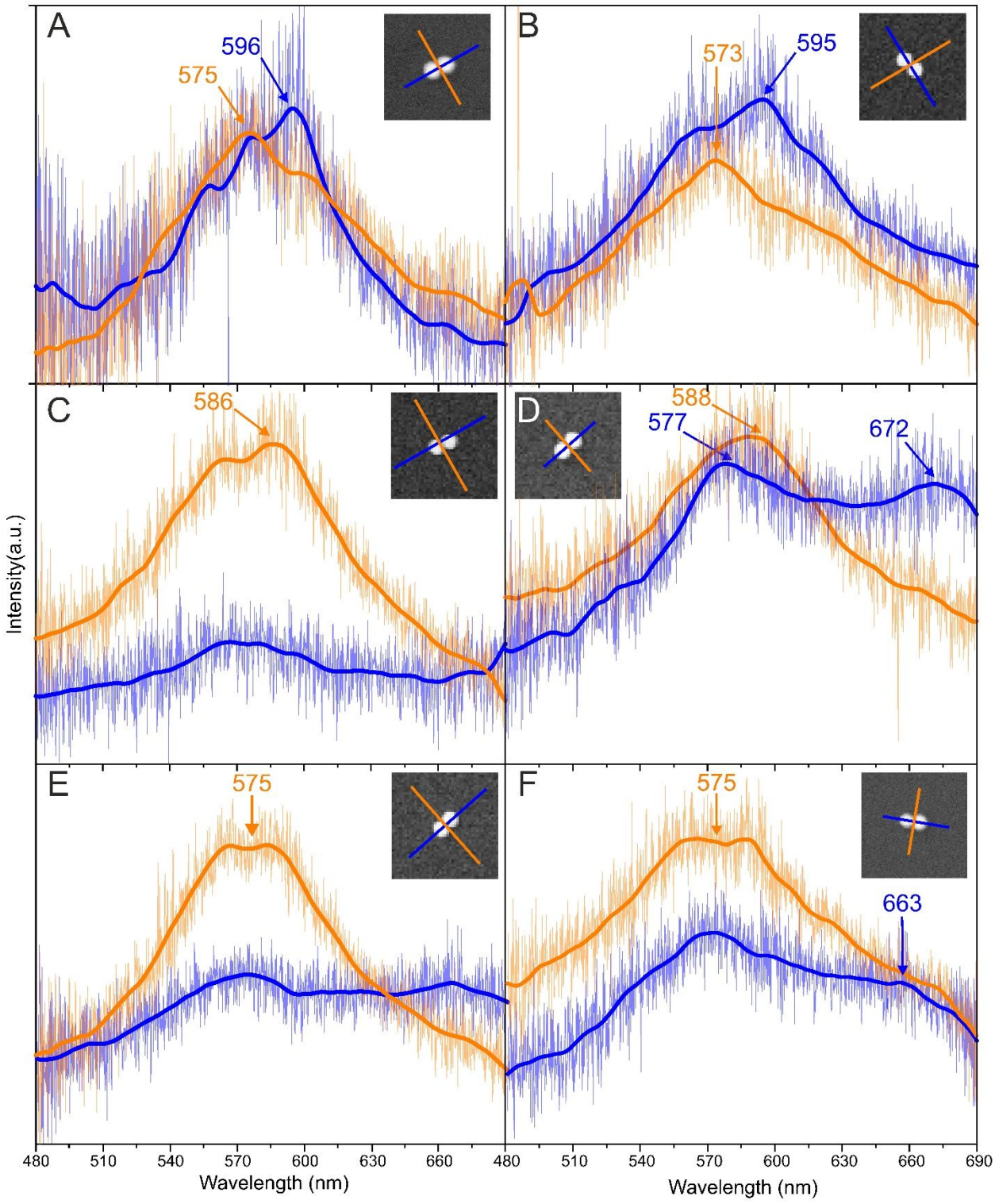

Figure S19. *Dark field scattering spectra of different DONAs. (A) – (F) DF scattering spectra showing the spectra along the gap axis (blue curve) and perpendicular to it (orange curve). The solid lines show an average fit whereas the real data is shown in the background. The arrows and the values highlight the position of the LSPR peaks.*

13. Time series SERS measurements in dark field mode

The time series data is measured from DONAs containing single Tamra molecule in the middle of the bridge. Typical Raman measurements were usually carried out by performing the Raman mapping first and then imaging the sample using SEM or AFM. However, since the dark field imaging directly visualizes the nanoparticles, we used it and AFM images to identify the dimers from the dark field view (see Figure S20). This was done by taking first a dark field image close to an external scratch marker, placing the same sample to AFM and imaging areas next to the same scratch marker. By using the same particle patterns in dark field and AFM images, maps were correlated (see the green rectangles in Figure 20A and Figure 20B for example). The sample was placed back to Raman microscope and the view was moved to the previously imaged area. Then we moved our internal laser reference point on top of any identified dimer (the red boxs in Figure 20 for example), turned the imaging mode back to bright field and acquired the Raman spectra. The power density of the used 633 nm laser was 5380 W/cm^2 and the acquisition time was 3 s.

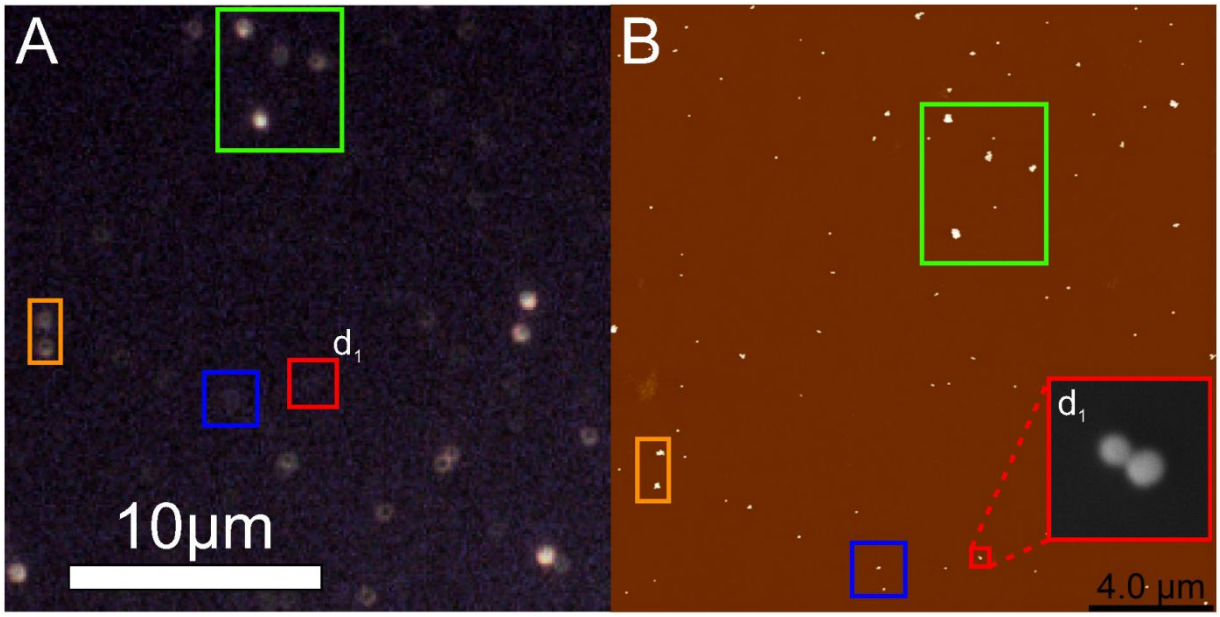

Figure S20. correlated dark field, SEM and AFM images of the dimer d_1 shown in Figure 4. (A)-(B), the dark field image after Fourier filtering and the corresponding AFM image from the same area. The scattering patterns highlighted by orange, blue and green boxes were used to identify the dimers from the AFM image. The dimer d1 from the Figure 4 is shown in the inset SEM image and highlighted by the red boxes in all of the images. The size of the SEM image in b is 300 nm × 300 nm.

Noise in the dark field images was reduced by creating a Fourier transformed image of the original dark field image, removing the center pixels (circular mask, 2-pixel radius) from the transformed image and doing the reverse Fourier transformation. For any image processing, ImageJ software was employed. The Figure S20A and Figure S20B show the dimer d_1 from the Figure 4 (red boxes in all of the images). Two other dimer time series spectra (dimers d_2 and d_3) are shown in Figure S21C and Figure S21D and the correlated dark field and AFM maps in Figure S21A and Figure S21B. Here, we can also observe fluctuations in the main Tamra bands of 1654, 1537, 1509, 1360 and 1216 (bands highlighted by the vertical, dashed lines).

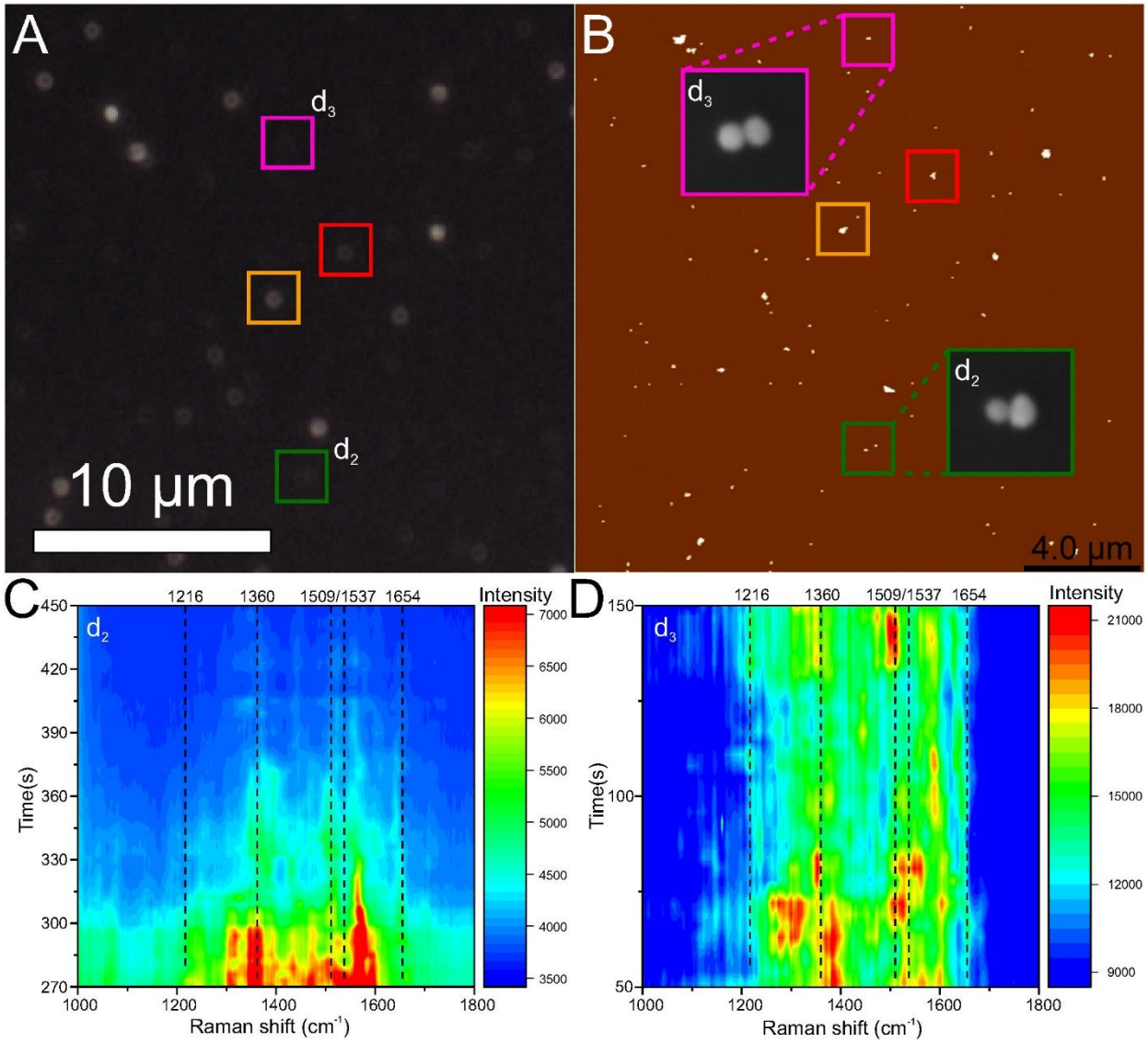

Figure S21. correlated dark field and AFM images of the dimer d_2 and d_3 area and the time series spectra of both dimers. (A)-(B) correlated dark field and AFM maps of the measurement areas. Red and orange boxes are used as reference to locate the dimers. The dimers d_2 and d_3 are highlighted by the green and violet boxes in all of the images, respectively. The size of the both SEM images is 300 nm × 300 nm. (C)-(D) time vs Raman shift contour plot for dimer d_2 and d_3 containing single Tamra molecule. The dotted lines indicate the main TAMRA peaks (1654, 1537, 1509, 1360 and 1216).

The intensities of the Tamra bands and fluorescence background decreased overall during the 600 s runtime (see Figure S22). This could be due to the measurement system going off focus during the relatively long runtime. However, for the dimer d_1, we plotted the time series of the main silicon peak at 520 cm^{-1} and observed no significant change in the peak intensity during the measurements, meaning that the initial focus on the surface was maintained during the measurements and the drop in the Tamra intensity might be due to changes in the morphology of the DONA samples: for example, it has been shown that laser power can be used to weld nanoparticles together.[2] These kind of effects might lead into

changes in the gap composition and the placement of the dye thus resulting in a drop in the Tamra peaks. Similar trends were observed in the case of dimers d_2 and d_3 (data not shown here).

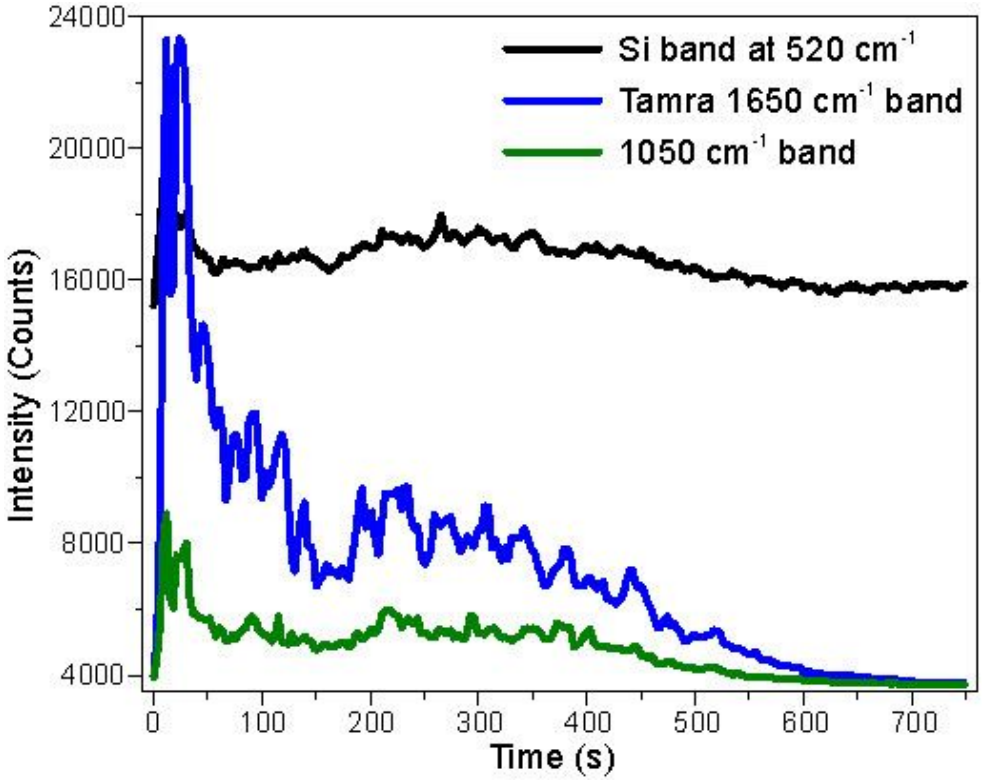

Figure S22. the dimer d_1 time series data of the silicon band at 520 cm^{-1}, Tamra 1650 cm^{-1} band and arbitrary 1050 cm^{-1} band.

14. Protein coupling schemes

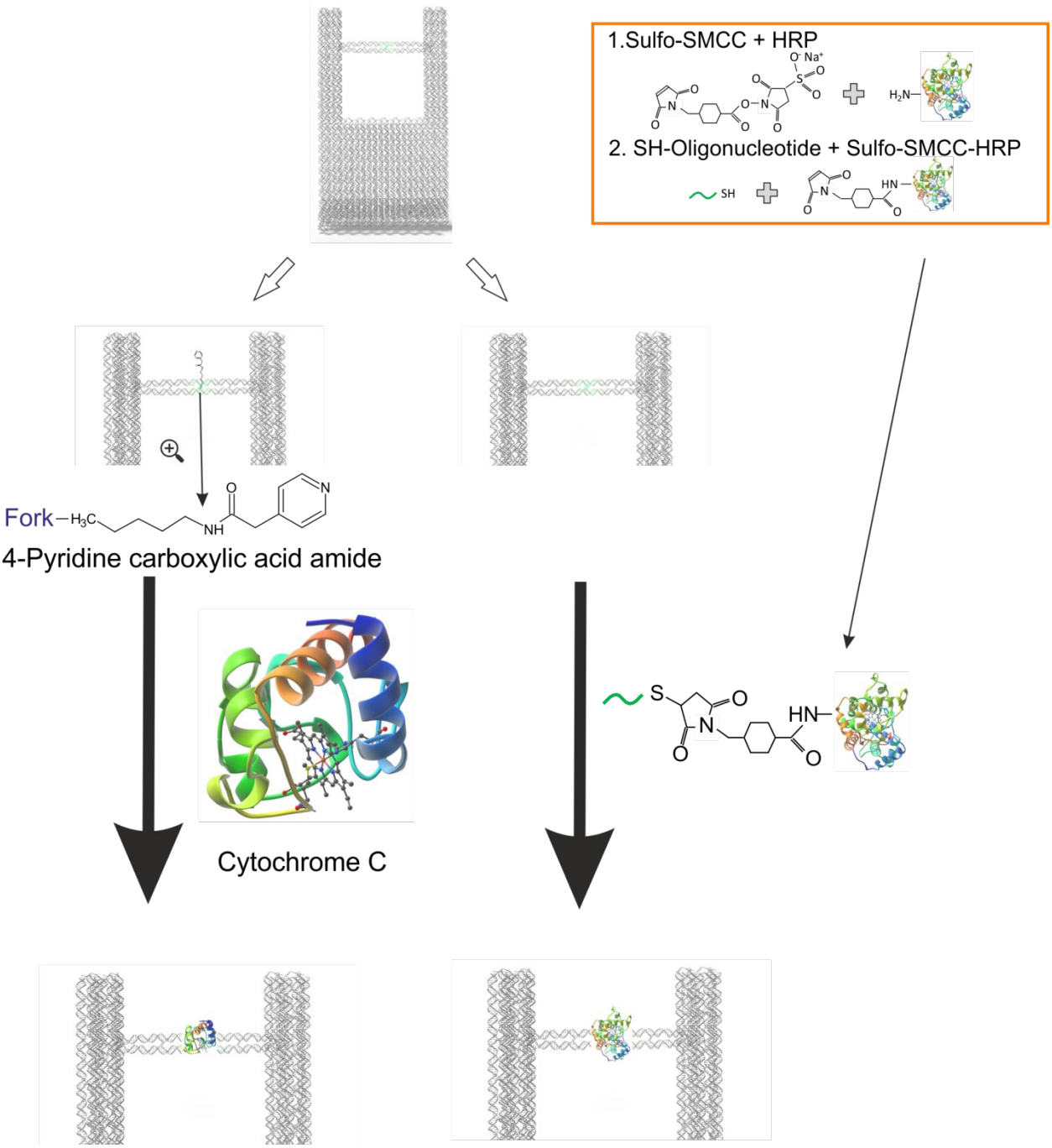

Figure S23. Scheme of the non-covalent and covalent coupling schemes to bind cyt c and HRP to the DNA bridge of the nanofork. Cyt c is coupled non-covalently to pyridine, which is connected to the DNA bridge, while HRP is cross-linked to a DNA staple strand, which is part of the DNA bridge. The cyt c and HRP models were adapted from [10.2210/pdb2B4Z/pdb] and [10.2210/pdb1HCH/pdb], respectively.

15. The correlated Raman-SEM maps of protein Au DONAs

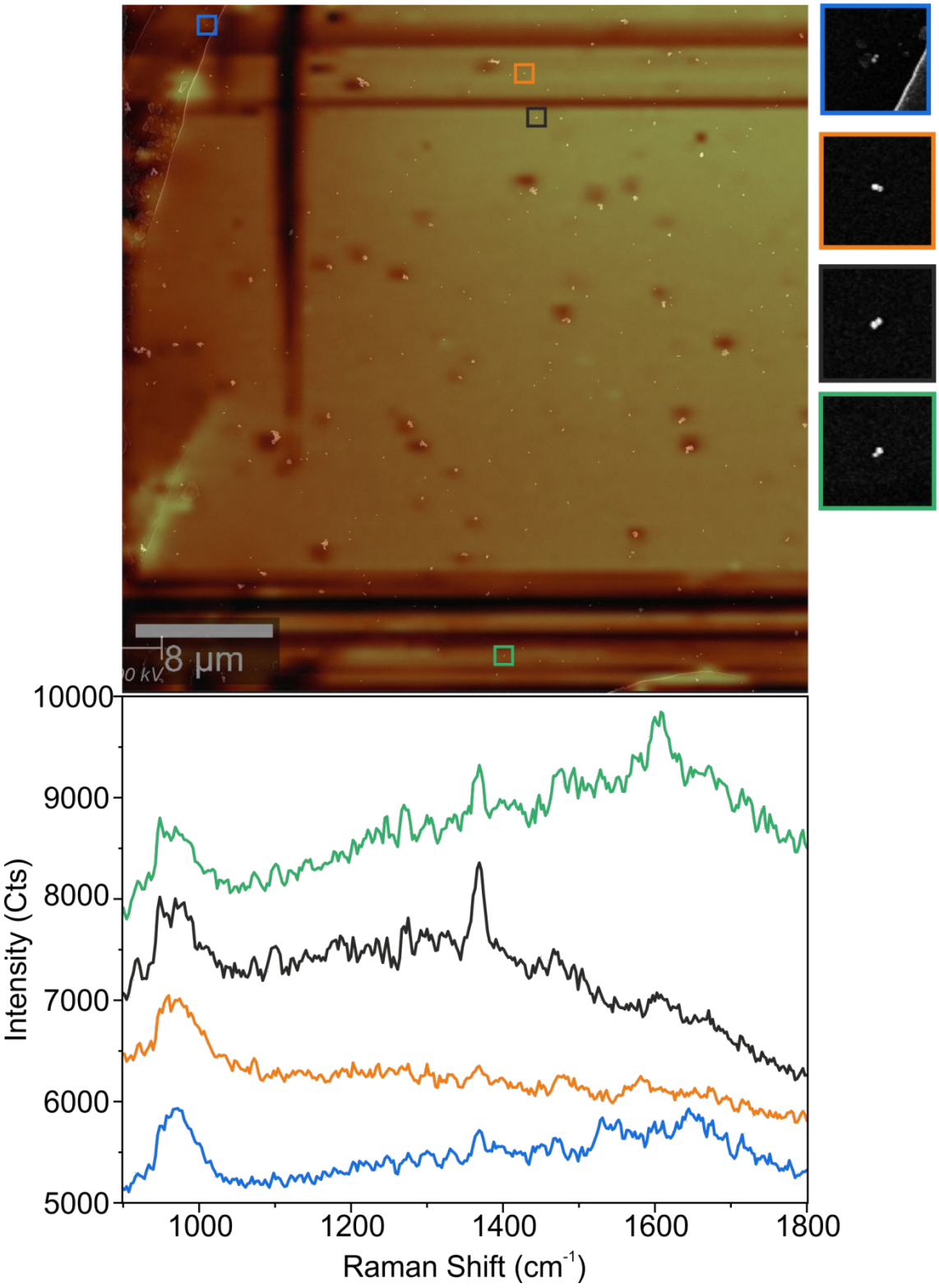

Figure S24. correlated SEM and Raman maps of Cytochrome C modified DONA-AuNP sample.

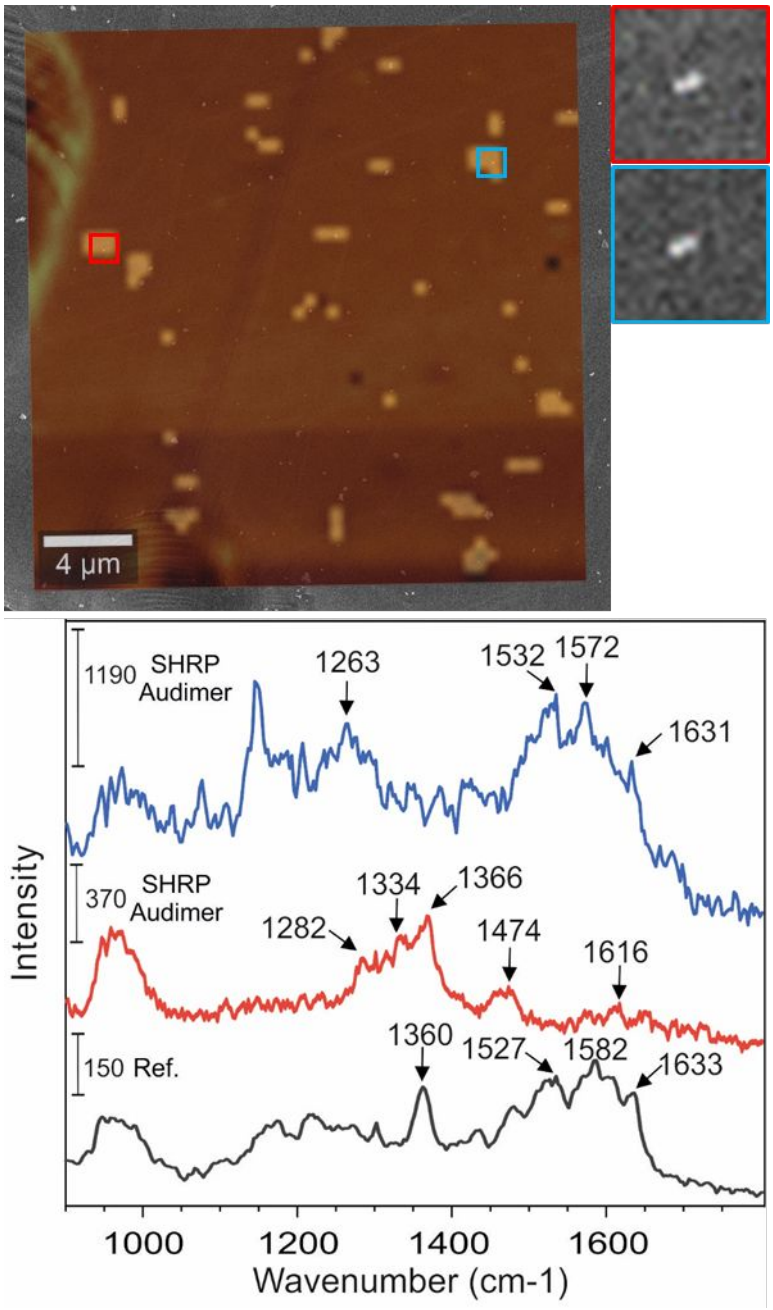

Figure S25. Correlated SEM and Raman maps of HRP modified Nano-Fork-AuNP sample. The colors and the number indicate the dimer areas (laser power: 200 µw, Integration time: 12 s).

16. SERS spectra of DONAs with unspecifically bound proteins

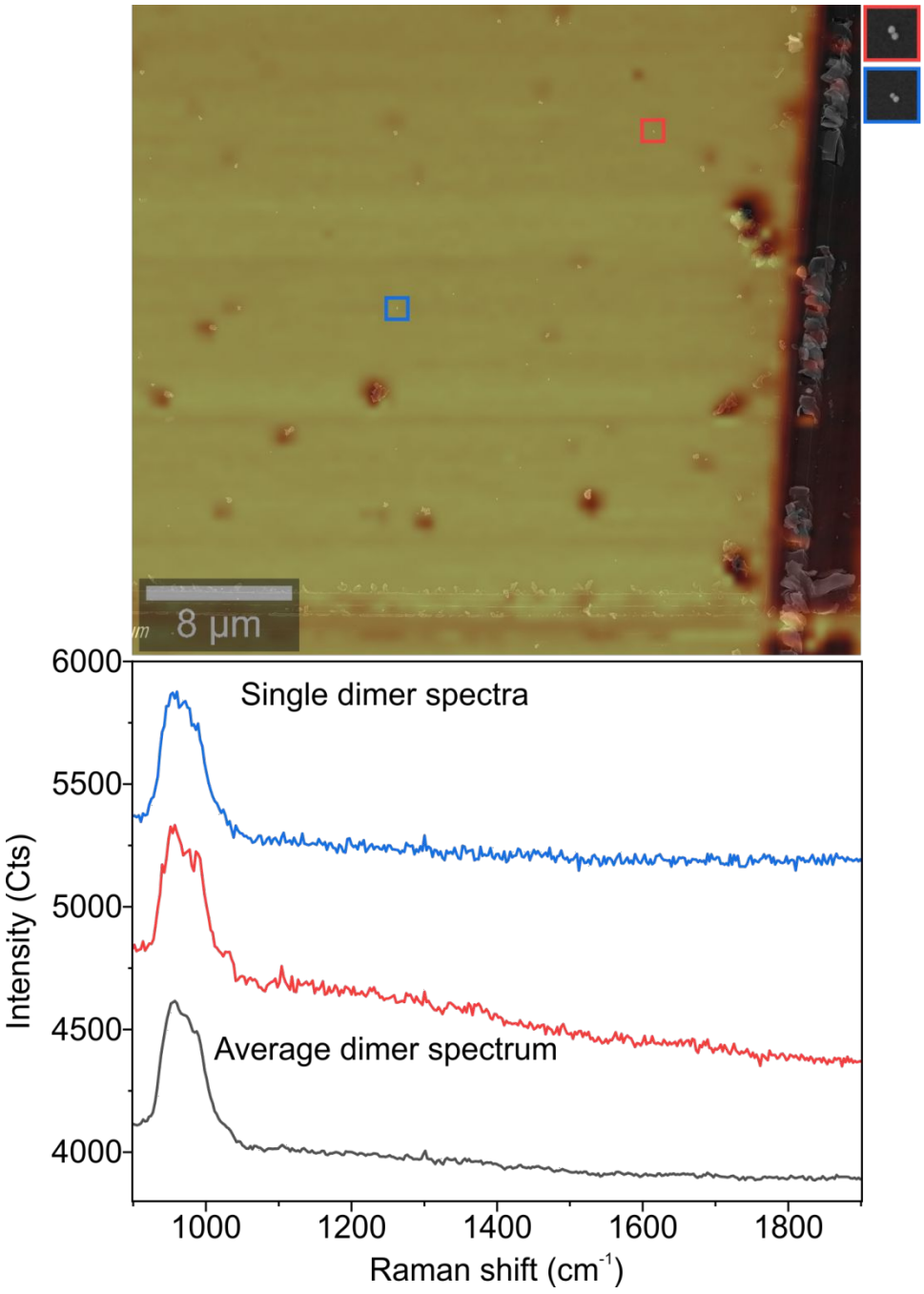

Figure S26. correlated SEM and Raman maps of control DONA-AuNP sample without Cytochrome capture strand.

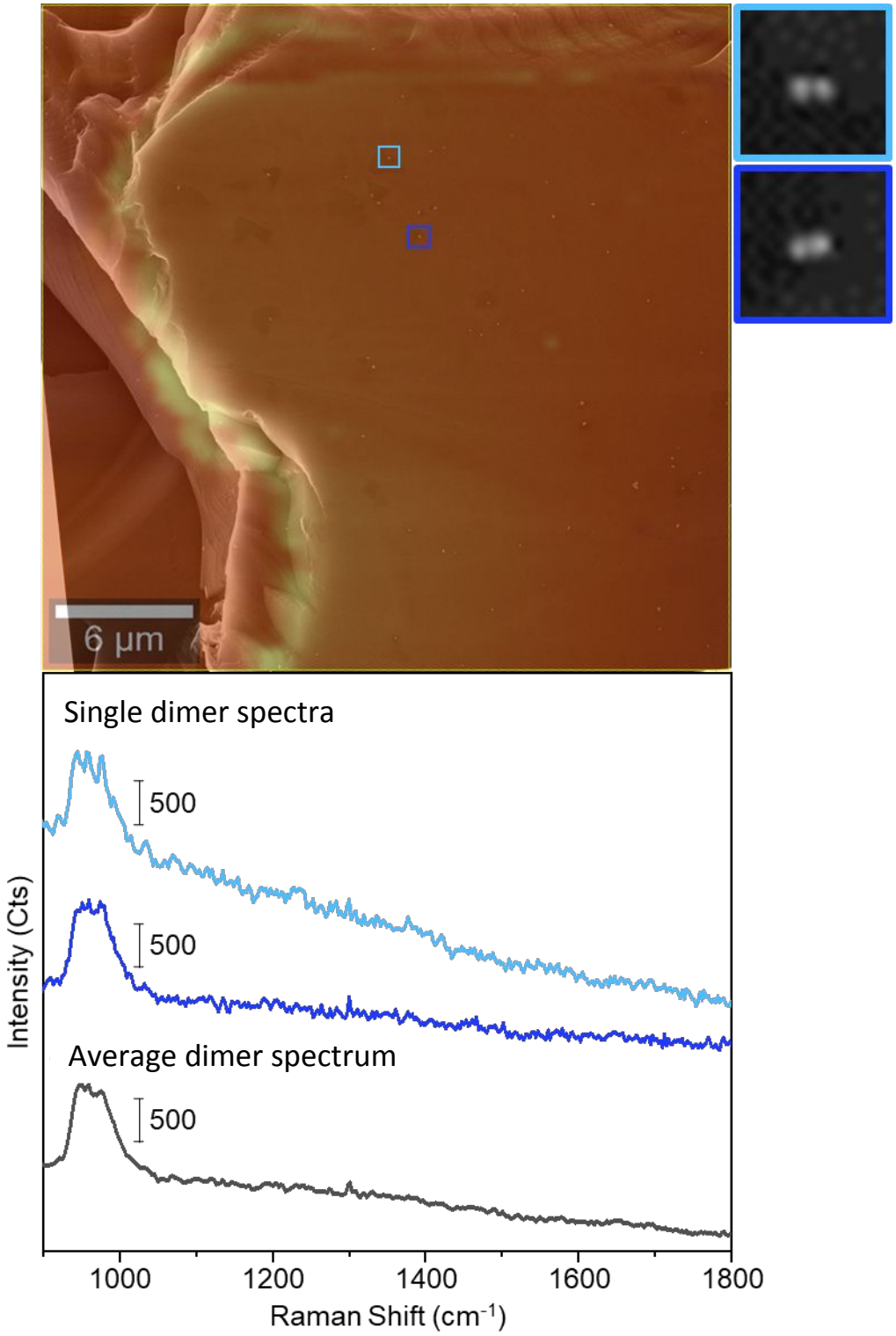

Figure S27. correlated SEM and Raman maps of control DONA-AuNP sample without HRP capture strand.

17. Example of Au and Ag DONA gels

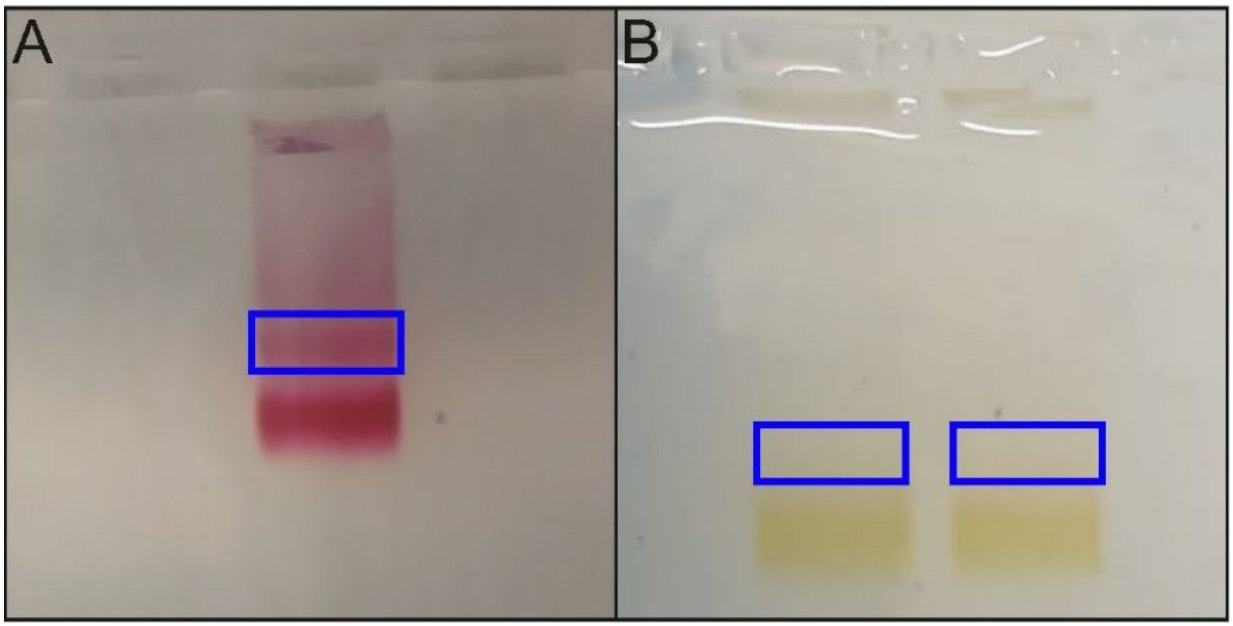

Figure S28. (A) and (B) depict the Au and Ag DONA samples after gel run, respectively. The blue rectangles highlight the dimer bands that are extracted from the gel.

18. Extra TEM images of DNA origami nanoforks

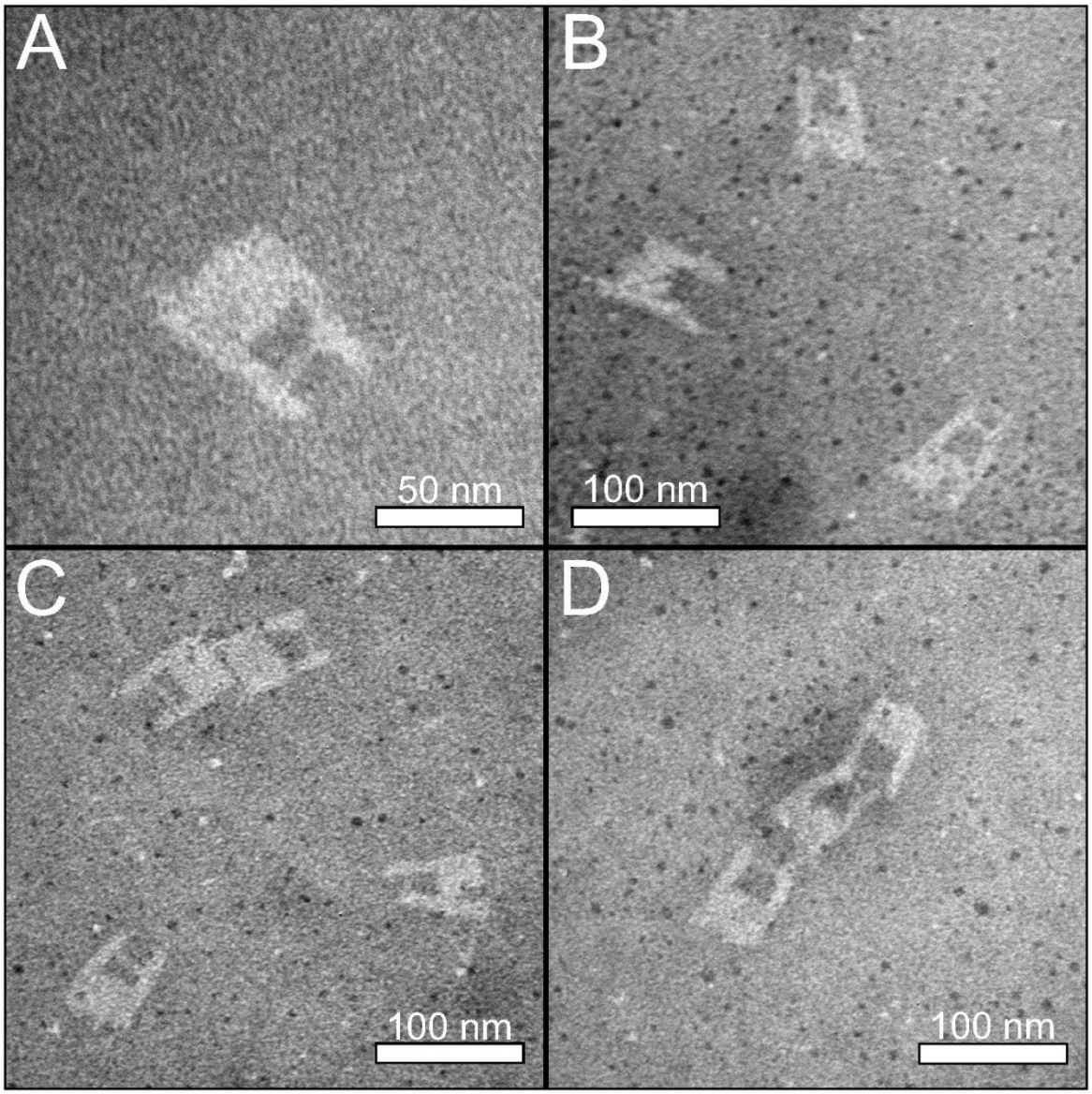

Figure S29. (A)-(D) extra TEM images of nanoforks on TEM grids.

19. Evaluation of the DNA coating layer thickness

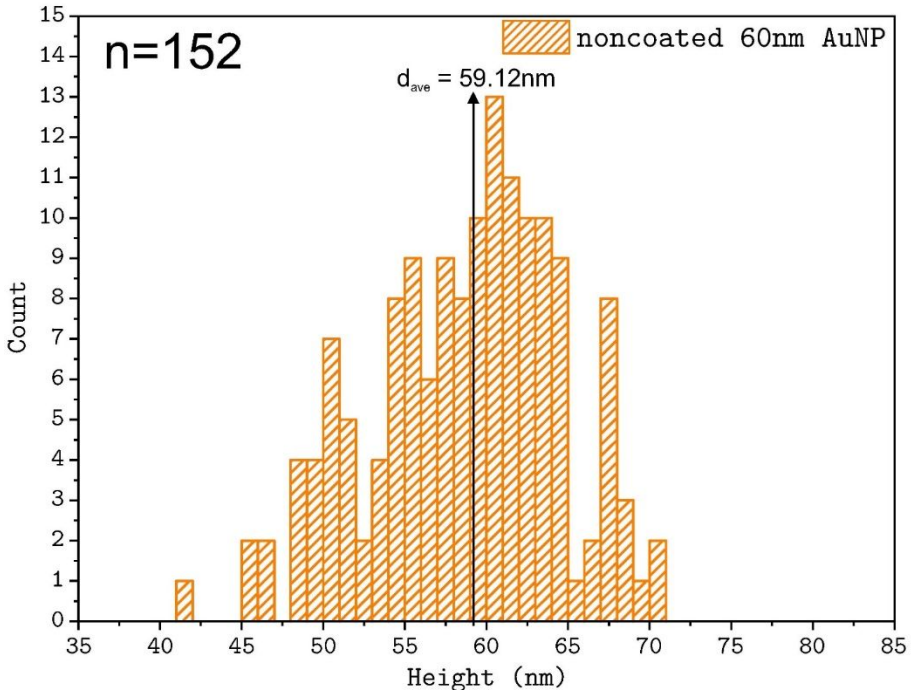

Figure S30. the height data of non-coated 60nm AuNPs (152 particles). The heights were acquired from AFM images.

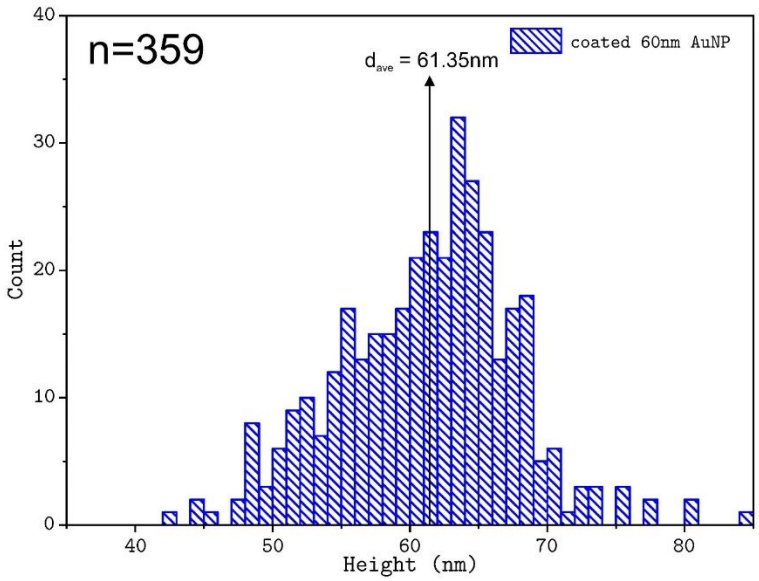

Figure S31. the height data of DNA coated 60nm AuNPs (359 particles). The height was acquired from AFM images.

The average DNA coating layer thickness was calculated from the average heights of the non-coated and coated 60nm AuNPs. Arithmetic averages were calculated (the vertical lines in Figure S30 and Figure S31) and the DNA layer thickness was calculated as the difference of the two average values divided by two, since the height value contains the DNA layer twice. This resulted in an average DNA coating layer thickness of 1.12 nm.

20. Plasmonic nanoparticle dimer simulations

The finite-difference time domain (FDTD) simulations were carried out using Lumerical FDTD Solutions software v8.19.1584. The model is shown in Figure S32. The gold and silver nanoparticles were defined as spheres with 30 nm radius and the refractive index (R.I.) of Ag/Au taken from Johnson and Christy.[3] DNA coating layers were placed on top of the particles surfaces, where the DNA layers were set 1.12 nm thick according to the average layer thickness in the previous section and the R.I. was defined as 1.7.[4] The substrate was Si (R.I. from [5]) with 3 nm SiO_2 layer (R.I. = 1.44) on top of it. The direction of the incident light was perpendicular to the surface and the polarization axis of the field was set either along the central axis of the gap (labelled gap mode, parallel to the blue source arrows in Figure S32) and perpendicular to this axis (labelled off gap mode). The simulation range was from either 350 - 650 (only off-gap Ag dimer simulation) or 400 - 850 nm and the step size was 1 nm. Overall mesh of 1 nm was defined throughout the simulated volume, except in the gap area a finer mesh was used: the mesh size was set to that between particles surfaces there were at least 10 elements (*e.g.* 2 nm gap equals 0.2 nm mesh). The finer mesh included the gap and a small part of the surface of each particle. Monitors were placed in the gap and outside to visualize and plot the E-field in respect to the position and the wavelength. The reference field E_0 was calculated by removing the particles and the coating layers.

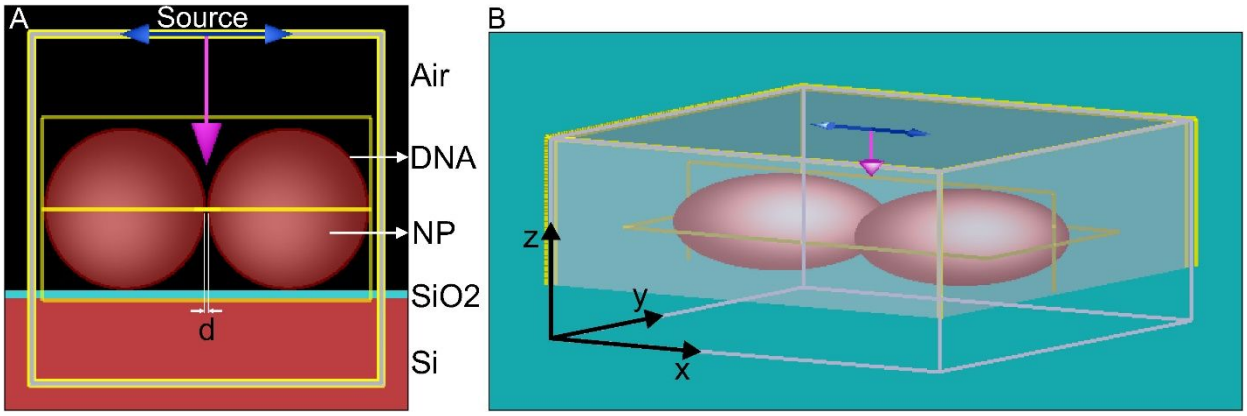

Figure S32. the model of DNA coated nanoparticle dimer on silicon surface used in the FDTD simulations. (A) the side view of the model. The dimer composed of two nanoparticles separated by distance d (np surface to np surface), where both have 1.12 nm DNA coating layer on top. The substrate is composed of 3 nm SiO_2 layer on top Si. The medium is defined as air. The polarization of the incident light (along the gap in the figure) is set either along the axis of the gap or perpendicular to it. (B) the isometric view of the same model. The x-, y- and z-axes are defined in b.

We varied the particle surface to particle surface distance based on the gap distribution in the Figure 1 (from 3.5 nm to 1.2 nm). Since the Lumerical model does not take into account quantum mechanical

effects, we restricted the gap distance to higher values than 1 nm to avoid effects like *e.g.* tunneling. We also defined water in the gap, when the distance between DNA layers equal or smaller than 0.75 nm, since it is less probable that there would exist a pure air gap between the DNA layers and rather the ambient moisture could form a water layer between the DNA layers in these distances. This means that gap size of 2.5 nm and 3 nm included a water layer (R.I. = 1.33) in-between the DNA layers. In general, the gold dimer had the predicted FE of 315 at 637 nm for 2.5 nm gap ($1.0x10^{10}$), 396 at 710 nm and 1.5 nm gap ($2.5x10^{10}$) and 601 at 736 nm and 1.2 nm gap ($1.31 x10^{11}$). For the Ag dimers, the predicted FE is 183 ($1.1x10^{9}$) for 532 nm excitation and a 2.5 nm gap, 473 ($5.0 x10^{10}$) for 633 nm excitation and a 1.5 nm gap, while the highest FE (621; $1.4x10^{11}$) is predicted to be at 664 nm for a 1.2 nm gap.

Figure S33 and Figure S34 show the field enhancement maps of the dimer gap region, when the distance between the nanoparticle surfaces is 1.2 nm, 2.5 nm or 3.5 nm and the excitation is at or close to one of the peaks in the FE curves in Figure 3. The highest field is always localized in the gap region with little or no visible coupling to the surface.

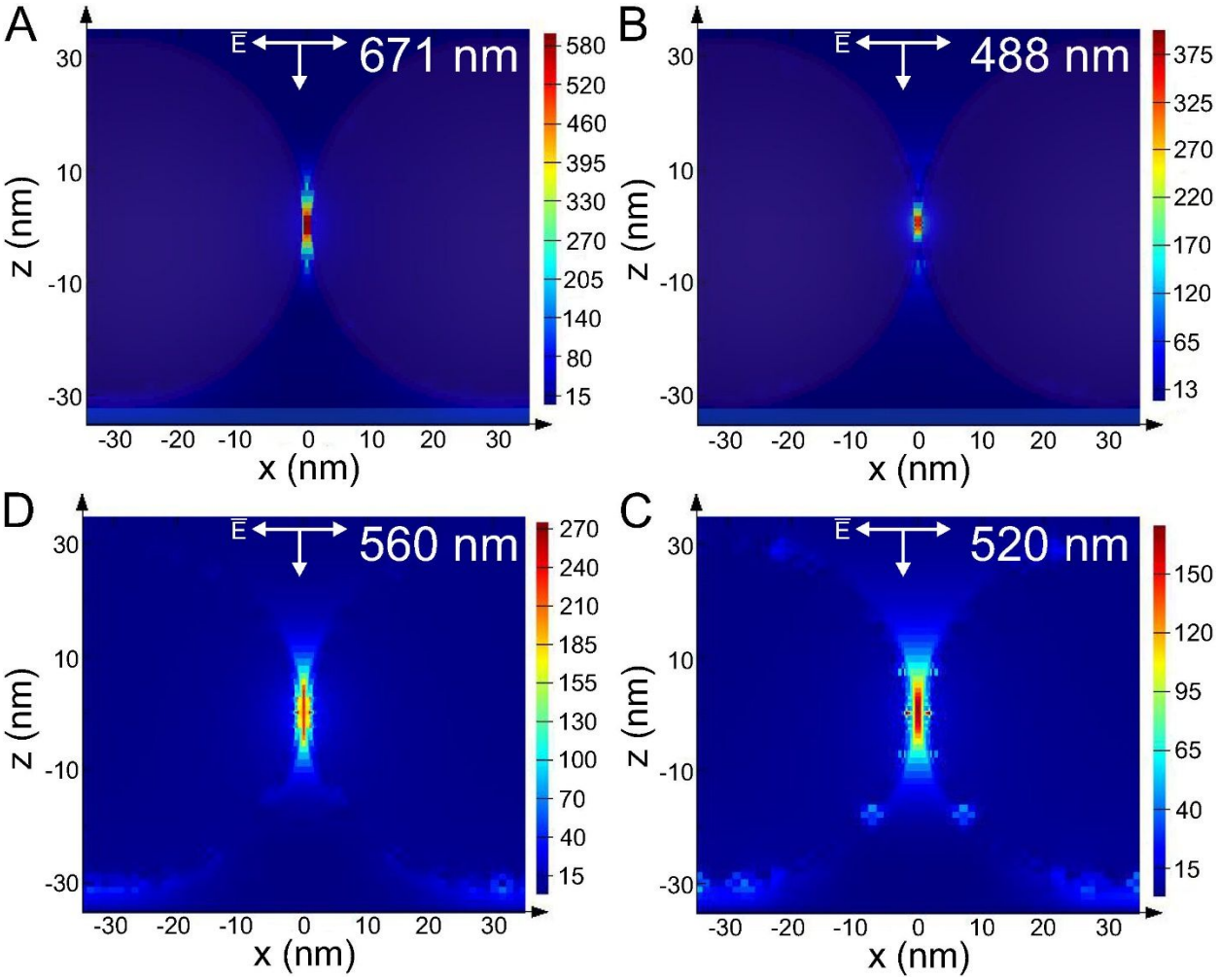

Figure S33. the field enhancement maps of Ag dimers at different excitation wavelength and gap sizes, when the polarization of the incident light is along the axis of the gap. (A) the side view FE map, when the gap size is 1.2 nm and the excitation is at 671 nm (the main peak for 1.2 nm gap in Figure 3B). An overlay of the FDTD model is added to highlight the particles and the surface. (B) the side view FE map, when the gap size is 1.2 nm and the excitation is at 488 nm (close to the second peak for 1.2 nm gap in Figure 3B). An overlay of the FDTD model is added to highlight the particles and the surface. (C) the side view FE map, when the

gap size is 2.5 nm and the excitation is at 560 nm (the peak for 2.5 nm gap in Figure 3B). (D) the side view FE map, when the gap size is 3.5 nm and the excitation is at 520 nm (the peak for 3.5 nm gap in Figure 3B).

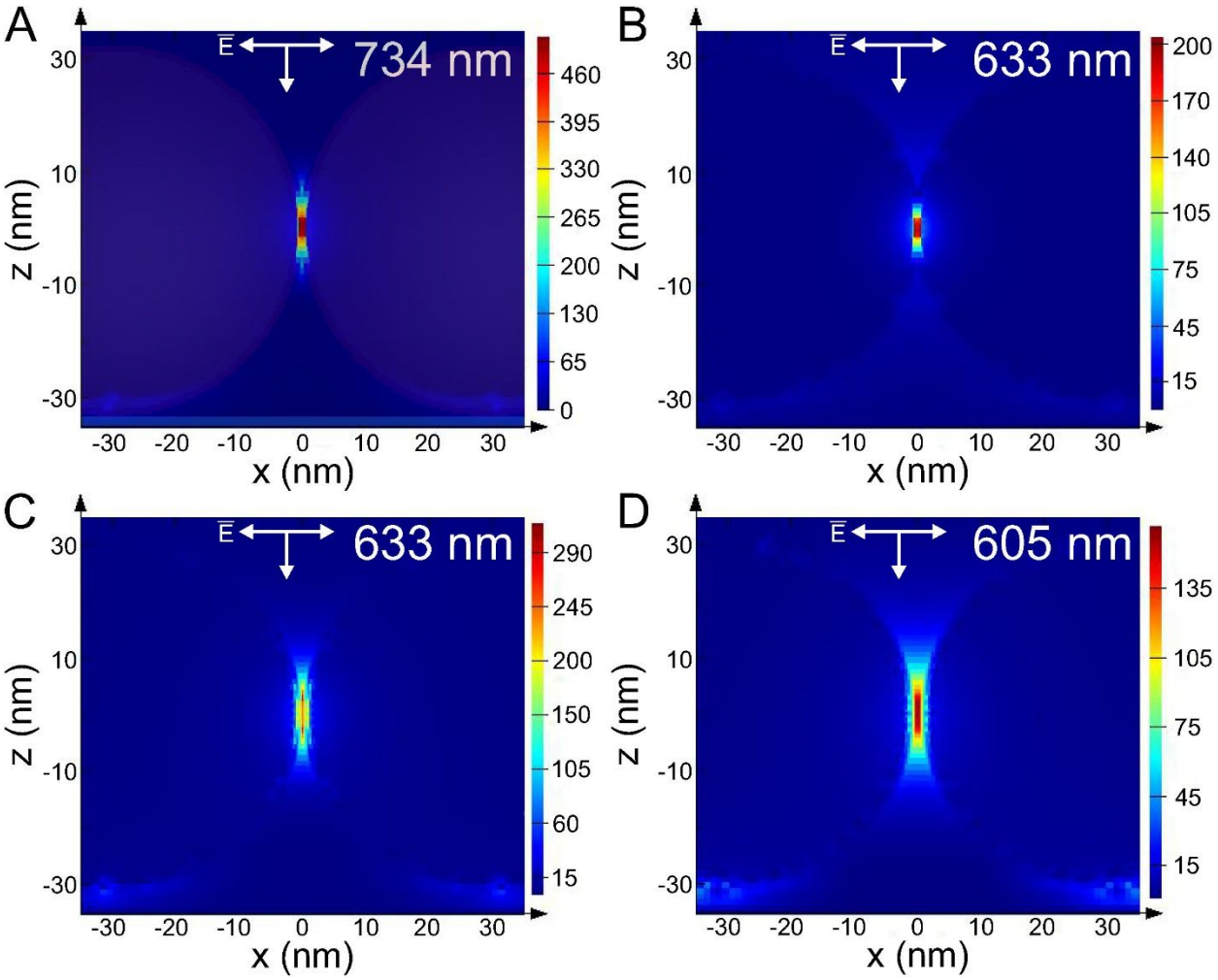

Figure S34. the field enhancement maps of Au dimers at different excitation wavelength and gap sizes, when the polarization of the incident light is along the axis of the gap. (A) the side view FE map, when the gap size is 1.2 nm and the excitation is at 734 nm (the main peak for 1.2 nm gap in Figure 3A). An overlay of the FDTD model is added to highlight the particles and the surface. (B) the side view FE map, when the gap size is 1.2 nm and the excitation is at 633 nm (close to the second peak for 1.2 nm gap in Figure 3A). An overlay of the FDTD model is added to highlight the particles and the surface. (C) the side view FE map, when the gap size is 2.5 nm and the excitation is at 633 nm (the main peak for 2.5 nm gap in Figure 3A). (D) the side view FE map, when the gap size is 3.5 nm and the excitation is at 605 nm (the main peak for 3.5 nm gap in Figure 3A).

The off-gap FEs for both AuNP and AgNP were also solved (see Figure S35, Figure S36 and Figure S37). The AgNP dimer off-gap spectra had the LSPR at 380.6 nm for 3.5 nm gap and redshifted slightly to 384 nm when the gap was reduced to 1.2 nm. For gold nanoparticles, the same wavelengths are 529 nm to 525 nm, respectively. This corresponds to the plasmonic excitation of single AgNP and AuNP. Notably, for the case of 1.2 nm gap and AgNP dimer, we observed an additional peak corresponding to coupling between silicon substrate and the NP at 366 nm wavelength (see Figure S36C). In the case of gold, no such additional modes were observed (see Figure S37B). However, these modes are not localized within the

gap region hence the FE in the gap is 1.95 – 2.77 for silver and 0.59 – 0.66 for gold dimer and we would not expect to detect single molecule spectra in these cases.

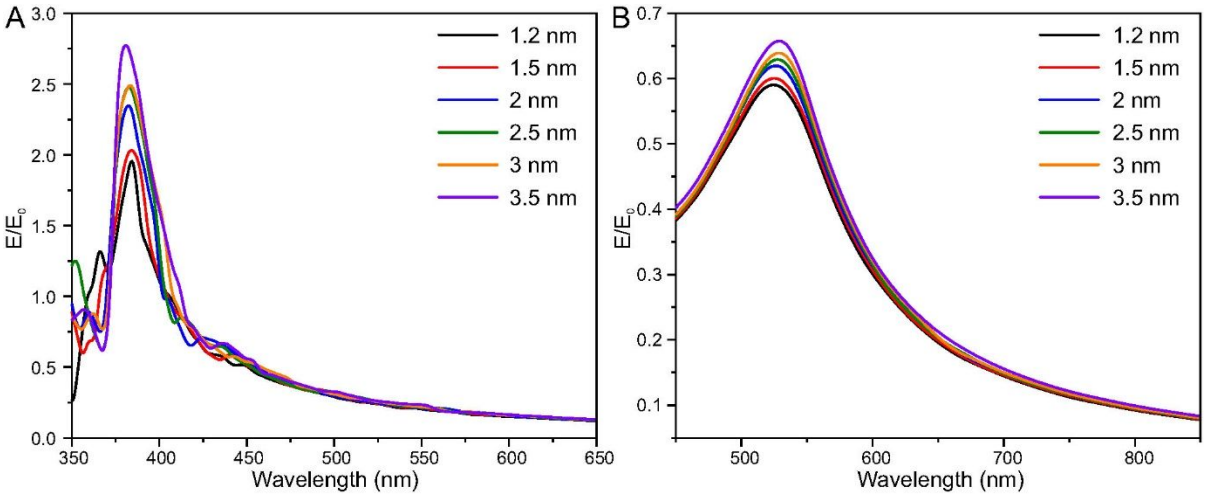

Figure S35. the field enhancement curve of Au and Ag dimers in respect to the gap distance when the polarization of the incident light is perpendicular to the gap (the parallel excitation is shown in Figure 1). (A) the field enhancement of Ag dimer, when the distance is varied from 1.2 nm to 3.5 nm. The peaks are around 380 nm, which corresponds to the LSPR of single coated AgNP. (B) the field enhancement of Au dimer, when the distance is varied from 1.2 nm to 3.5 nm. The peaks are around 530 nm, which corresponds to the LSPR of single coated AuNP. The field values are extracted from the middle of the gap region in all of the cases.

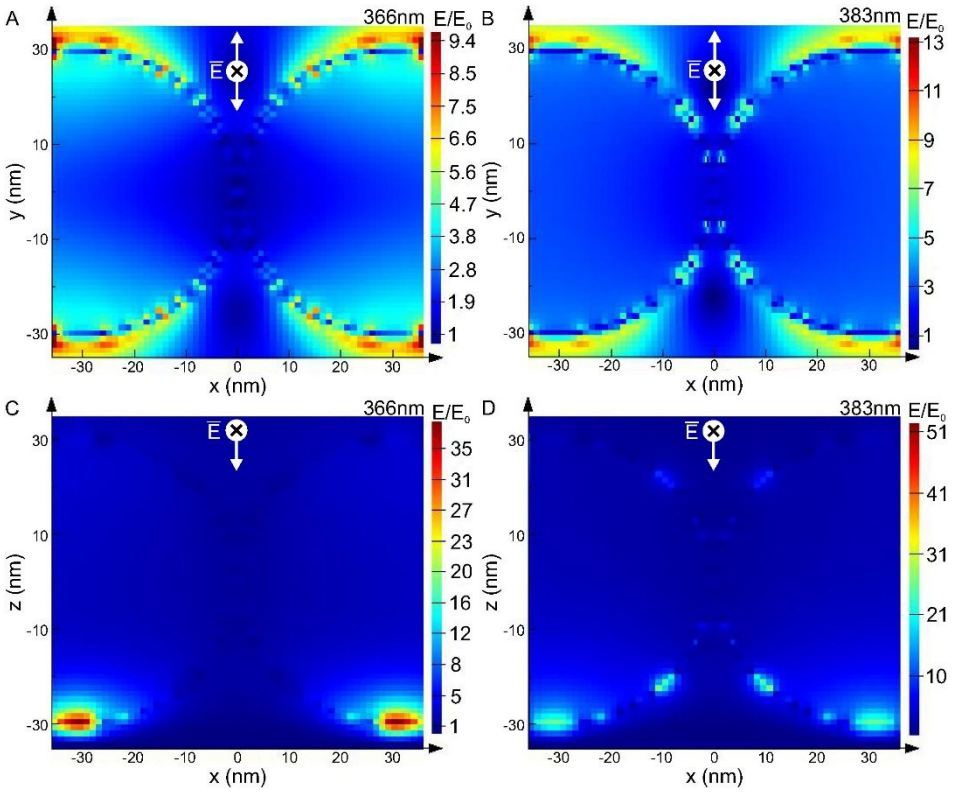

Figure S36. the field enhancement maps of the Ag dimer at different excitation wavelengths, when the gap size is 2.5 nm and the polarization is perpendicular to the gap axis. (A)-(B) the top view FE maps when the excitation is at 366 nm and 383 nm, respectively. (C)-(D) the side view FE maps when the excitation is at 366 nm and 383nm, respectively. The silicon substrate is at the bottom of the C and D figures. The excitation at 383 nm corresponds to LSPR of the single coated AgNP, whereas the 366 nm excitation seems to include coupling to silicon substrate as well as the dipole excitation.

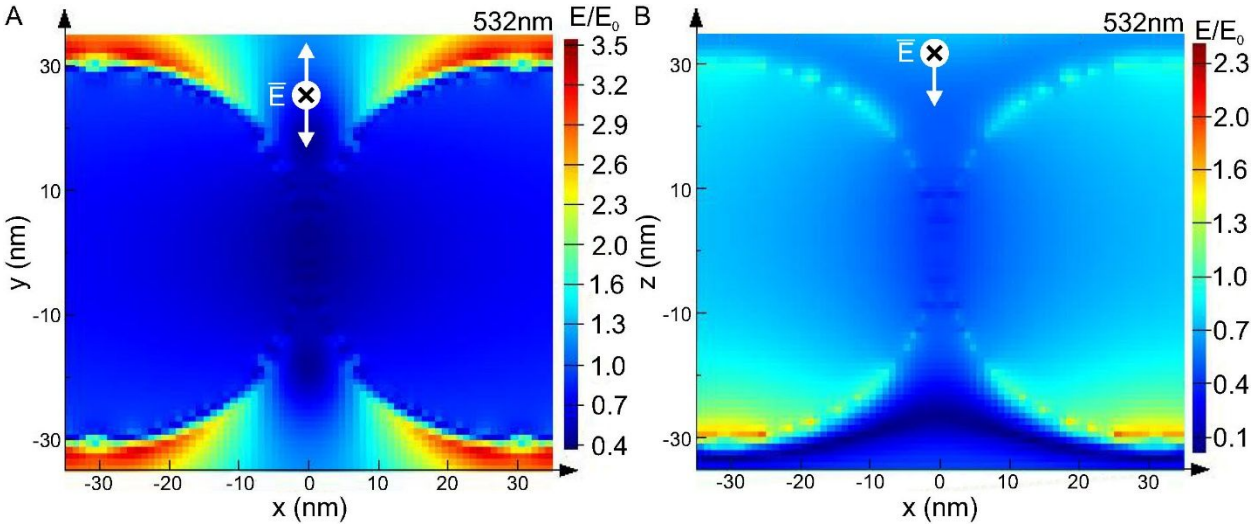

Figure S37. the field enhancement maps of the Au dimer at 532 nm excitation, when the gap size is 2.5 nm and the polarization is perpendicular to the gap axis. (A) the top view FE map when the excitation is at 532nm. (B) the side view FE map when the excitation is at 532 nm.. The silicon substrate is at the bottom of the B figure. The excitation corresponds to LSPR of the single coated AuNP with some coupling to the silicon substrate.

21. The calculation of the hot spot volumes

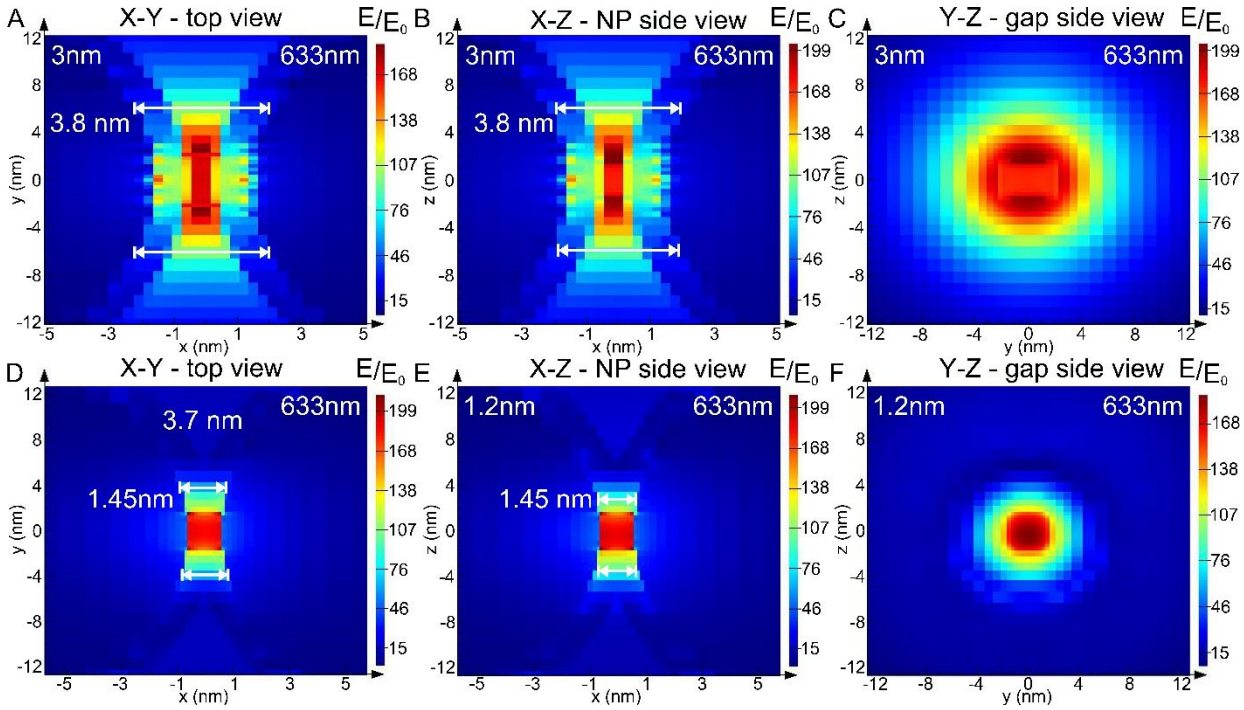

Figure S38. the field enhancement maps of the hot spot of the Au dimer at 633 nm excitation, when the polarization is along the gap axis. The hot spot is defined as a volume, where $\left(E/E_0\right)^4$ *is roughly 10⁸ - 10⁹ or* E/E_0 is 100-178. *(A)-(C) the top and the two side views of the hot spot around the gap area, when the gap size is 3 nm. The white arrows indicate the border of the hot spot volume. The hot spot volume resembles roughly a concave lens with the radius of 3.75 nm, the width at the edges of 3.8 nm and the width at the narrowest region of 3 nm. The total volume is then 159 nm³. (D)-(F) the top and the two side views of the hot spot around the gap area, when the gap size is 1.2 nm. The white arrows indicate the border of the hot spot volume. The hot spot volume is approximately a cylinder with an ellipsoidal cross section, where the length of the cylinder is 1.45 nm and the diameters are 2.8 nm and 3.02 nm. The total volume is then 38.6 nm³.*

22. List of modified DNA origami nanofork strands

Table S1 – The list of the modified nanofork strands

Strand	Strand# in Table S1	Sequence	5' end Mod.	3' end Mod.	Supplier
S173-NP cap.	173	AAA AAA AAA AAA AAA AAA AAA AAA AAA GGG AGC CCC CGA TTT AGA GCT TAA ACC TGT CGT GCC AGC TGC ATT AAA ACA ACA ACA ACA ACA ACA AC			Metabion
S129-NP cap.	129	AAA AAA AAA AAA AAA AAA AAA AAA TTT TTG GGG TCG AGG TGC CGT AGA GGC GGT TTG CGT AAT GGG AAC AAC AAC AAC AAC AAC AAC AAC			Metabion
S161-Cy5	161	Cy5 - TTT TAA AGC ACT AAA TCG GAA CCC TTG AAT CGG CCA ACG CGC GGG G	Cy5		Metabion
S161-Cy3.5	161	Cy3.5 - AA AGC ACT AAA TCG GAA CCC TTG AAT CGG CCA ACG CGC GGG G	Cy3.5		Sigma Aldrich
S161-Tamra	161	Tamra - TTT TAA AGC ACT AAA TCG GAA CCC TTG AAT CGG CCA ACG CGC GGG G	Tamra		Metabion
S161-4-P-AA	161	4-Pyridine acetic acid - C5 – TTT AAA GCA CTA AAT CGG AAC CCT TGA ATC GGC CAA CGC GCG GGG	4-Pyridine acetic acid - C5		Biomers
S161-thiol	161	AAA GCA CTA AAT CGG AAC CCT TGA ATC GGC CAA CGC GCG GGG TT - C3 - Thiol		C3-thiol	Metabion

23. List of DNA origami nanofork staple strands

Table S2 – The list of the general DNA origami nanofork strands

Strand#	Start	End	Sequence	Length
1	41[147]	35[150]	TTTGACCAGCGGATAATCAAAAGTTCAGGTAATAGTGCAAAACTCG	46
2	8[233]	8[215]	TATAAGTATAGCCGCCTGT	19
3	47[54]	40[56]	AAATTTTTATACCAAACCCACTACAGTGAGCGGAAGCAAACTCC	44
4	60[173]	65[178]	CACGACGAATTCGTTGTTATTTATTAATCGTATTACATTTTGACG	45
5	82[233]	49[233]	GTGCCACGTAGACCGTGTGA	20
6	27[172]	22[168]	CGGGACAGATTTACTTAGCCGCCGCTCTGAATTGCGAA	38
7	23[151]	63[139]	AGACGTTGAAAATCTCCAAAAAAATAAATCCAAACAGGGAGCACG	45
8	42[181]	47[173]	AGCCTAACTCCCGAAGAACGGGTATTAAAATGCAGTTCGAGCACCGTT	48

9	35[138]	38[138]	ATCAATAGGATTGTATAAGCAAAAGCCCCAAGAGGGGAAAACGAGA	46
10	40[124]	45[118]	AGCCCGAAAGACTTCCACGCCAAAGAACATCCAA	34
11	26[160]	59[160]	GTACAGAAGTAATCAACGACGATTAAGT	28
12	22[209]	63[202]	AGCGGAGTGAGAATATACATGTATTAGATATCATT	35
13	40[41]	40[17]	AGAGAGTACCTTTAATTGCTTTTTTTT	27
14	51[174]	37[187]	GTTAAACTTAGGTTGACTAGCATACTGC	28
15	2[233]	2[215]	CACCCTCAGAGCATGTACC	19
16	56[233]	11[233]	AGATGATGAATTATCACAGGGCGATTTGCTCAGT	34
17	41[23]	43[41]	TTTTTTTTTCCTTTTGATAATTTTGCGGGTCAATAACCTGTTAGATACTTAATTG	55
18	42[141]	45[137]	GAAATCGGCGGCTTATCAAGCCGTTTTTATTAAATTCTGTCC	42
19	44[48]	47[53]	TGACCATTTAGCTATGACCCTACGCAAGGATAA AACAACAACAACAACAACAACAAC	57
20	21[215]	21[235]	ATGGGATTTTGCTACGGGGTC	21
21	40[139]	48[131]	AAAAGATAGGCGAAAAAAGGTAAAGTCAGAAAGGCGG	37
22	38[202]	47[202]	ATAGCTAATCAGAGCATAATTTATACAA	28
23	91[25]	90[25]	CGTGAACCATCACCCAAATCAAGTCGCCAGGGTGGTTTTTCTTTTCAC	48
24	49[182]	40[182]	GTAATCGAAAGCCTAATTGAGAACACCC	28
25	43[17]	44[17]	TACATCATGGCTTAGAGCATTTCGCAATTTGATGTA	36
26	30[163]	55[160]	TGGTTTAATTATTTTAAGTATCGGGGCGCAT	31
27	39[138]	41[146]	ATCTACAAACGGAGACAGTCAAATACCGACAATCCTG	37
28	63[140]	26[138]	TATAACGATACGAGTGTGTCGCATAGGCTG	30
29	29[138]	32[138]	CCCAGCTGGGCTTTCCGGCACCGAAGATCGAATTACCCAGGTAGAA	46
30	22[83]	63[76]	AGGTGAATTTCTTAAGGCCGCTTTATAAGTAACCA AAC AAC AAC AAC AAC AAC AAC AAC	59
31	37[138]	40[140]	ATCACATCGCCATTAAAAACTGAGAGCCAGATGTA	36
32	28[160]	57[160]	GCTCATTCAGAACGCGGGCCTTGCCGGA	28
33	43[42]	42[15]	CTGAATAGTGGACTCCAACGGTCATTTTTGCGGTTTTTTTT	41
34	32[160]	35[166]	GAACAACATTTAGGTGGGAACTGGCCTTCCTGTAGTTTTTGTGACGAT	48
35	42[97]	40[104]	AGGGTTGCGGTGTCTGGAACGCCCAATAGAATAGCCAAGCGGTCAAATAT	50
36	36[181]	49[181]	AAAAGAACGTCCAATGTCAATATGAACG	28
37	65[91]	24[98]	TATCGGCCTTGCTGACGGTACAGCAGCGTACAGAG	35
38	44[195]	49[199]	TCCTTATTCAACAATGTAATTTATGCGTACTAGAATATCTTCTGAC	46
39	51[221]	81[241]	ATCACATCGCCATTAAAAACTGAGAGCCAGATGTA	35
40	46[233]	1[233]	GGCTTAATTGACAGAGAGCTACAACCACCCTCAT	34
41	50[212]	55[213]	AAATGCTGATAATCATAAGCTTAGCGCTATTATAA	35
42	30[181]	59[173]	CCATTACTACCAGTATGTTTGAGGGGACCAAAGCGAAGGGCGCGCCAG	48
43	65[116]	22[126]	AACAATATTATTAAAGGAATTCACAAACAAAAGGCTCC	38
44	22[125]	63[118]	AAAAGGAGCCTTTAGCATCGGGATTTTAGCGTACT	35
45	38[160]	47[160]	TTTAAACAATCAGGGGGTAGCCAATATG	28
46	20[233]	20[215]	TGCCTTGAGTAATTTCTGT	19
47	51[203]	38[203]	ATGTAAATATATTTCCCTTTTAATAGCA	28
48	45[138]	42[142]	AGACGACGAGAACAAGCCGGTATTCTAAGAAGTGGTGGTTCC	42

49	24[202]	65[195]	CAGAGCCTCAATCACAATTCATCAATTGGTAACATCTTTACATGAAATG	49
50	63[182]	60[174]	AGTTTGATTTCCTGCGAGGCGCAACTTTGAAAGAGATATTCATACCCAGT	50
51	62[48]	65[48]	AAAGGAAGCTGGCAAGAGTCTCTTCTTT	28
52	3[215]	45[233]	GTAACACCCAAACAGGAGCCTTTAGAATCGAAATAATATCCCATCCT	47
53	32[213]	26[211]	ATTGTCATTAATTTGGGATAGCAGCCTTTAGCGCGTTTGGAGCCA	45
54	59[213]	65[216]	TAACTTATTTGTTATACTTTATCAGACAAAGATGAGGATGCAGATT	46
55	24[55]	62[49]	AAA AAA AAA AAA AAA AAA AAA AAA AACGGGTGAATACATGGCGAG	45
56	59[161]	27[171]	TGGGTAAATCGGTGAGTAGTAAATTGTTAACGTAAGAAC	39
57	61[161]	28[161]	CGAGCTCGTTGTAATTGACAACAAAGCT	28
58	35[167]	30[164]	AAAAACGGGCCAAAACATTCAAAAAACGACTCATTACAGGCTTGAGA	47
59	57[182]	28[190]	CCATTCACAATTTCCAGGACGTTGGGTAAATCACCCGTCACCCGTTTT	48
60	18[233]	18[215]	AGTTAATGCCCCGTTAGTA	19
61	12[233]	12[215]	AGGATTAGCGGGATAGTTA	19
62	25[42]	22[15]	GGCAAAAAAAATACTCGGTCGGCGCCGACAAT GACAACAACCATCGCTTTTTTTT	55
63	53[182]	36[182]	CATTAAAAACCTCCAAGACTCAATACCC	28
64	40[181]	43[188]	TGAACAAATAAGAAAGGCATTAACGCGCCTGTTTACATTCCACTTGCGG	49
65	61[221]	71[233]	AATCCCTTCTGACCTGAAAGAAAGGAA	27
66	45[98]	47[90]	AGTAGTACGGTTTCATTCCATATAACAGTCAATTCGCCTCAGGCAATGC	49
67	49[161]	36[167]	AAACAAGCCGGAGATCTTTACCCTGATCTCCCCCTTGGATAGCTCAAAAT	50
68	40[55]	45[55]	AAAAAAAAAAAAAAAAAAAAAAAAAACAGGTAAAACCGAACATTATATTTTC	52
69	59[174]	30[182]	GGTTTTGATTTTCAGGCGCAACCCGGAAAAGTAGCA	36
70	26[210]	59[202]	CCACCGAGGGAACCGTAGCCCCAACAGAAGTCAGAT	36
71	35[151]	30[150]	TTTTAGTAAGAGTTGAGATTATTATTATGCGTCAA	35
72	70[233]	61[233]	GGAAGGTTAAAATGGAAGGG	20
73	6[233]	6[215]	ACCGTACTCAGGAGTACAA	19
74	63[153]	26[161]	CCTCGTGCCCGAACGCCGCTCACTCCATGGAACGGT	36
75	57[151]	63[152]	TGGCTTCGCTCAAGGCGGCCAGTGGGATCCCACACAACTGCTTT	44
76	27[190]	22[185]	CGGTCAAACTGACCAGACGGGCCACCAAAGCGTCAGAAAGGAACA	45
77	55[214]	59[212]	ATCTCAAGAATATTCATCTGATTGCAG	27
78	25[21]	62[21]	TACATCACCAACCTAAAAAAGCGAAAGTTTGATGTA	36
79	68[241]	63[241]	TACATCTCTTTAGGAGTCAGAAGGAGCGGAGATGTA	36
80	11[215]	53[220]	AGCCCTCGTCATTCAAACCAGCGAAATCGTATTA	34
81	45[119]	40[125]	TAAATCATTTCATCAATCAGATATAGAAAAAATCCCCCCAGCTAAGAGGA	50
82	49[221]	83[233]	ACCCCGAACGAACCACCAGCCGCCTGC	27
83	43[189]	38[183]	GAGGTTTGAGCGTCTTTGTTTTTAACTGCGCTAATTCGTCATAAATAT	48
84	59[221]	73[233]	CCTGTAAGAATACGTGGCACAGTTGGC	27
85	40[103]	45[97]	CGCGTTTTAATTCTGAGAGACAATAAATACTAAT	34
86	34[202]	51[202]	CACCACGCGCAGTAGAGACTATAACTAT	28
87	50[196]	53[200]	ATTTCAAAGGTTATACCTTTTTTGTCCTTGAAAA	34
88	22[103]	63[97]	GGTTTATCAGCTTCACCCTCGCCAGAACTTAATG	34
89	63[77]	22[84]	CCACACCATTGCGTCCCAGCGATTATACGGACTAAGGATCGTGCTTTCG	49

90	65[20]	24[18]	TTTTTTAACCGTTGTAGCAATAGTCCATCGATATATGTAATGCCACT ACGAAGGCTTTTT	60
91	47[221]	85[233]	CCAGAAGATAAAACAGAGGTGAGGCGG	27
92	55[221]	77[233]	TATCTATTAGTCTTTAATGTGCTGAAC	27
93	44[216]	50[213]	CAATCAAACAAGAACCATATTCCAGTATATAAACATGGTTTGTTTC	46
94	65[140]	24[140]	AACAGGAGGGAGCTTCATTAAGGCAGGT	28
95	47[161]	44[154]	ATATTCACAGTAATTTATCCCGTTACAAAATAAACACGCGAGACCGCAC	49
96	24[139]	61[139]	CAGACGAGATAAATCCGGAAGAGGTCGA	28
97	42[76]	44[70]	TTGGAACTTTAAATCCAATTC	21
98	42[118]	47[111]	ATCAAAAGCAAGCAGTAGGAATCATTACGCATTAATTAGCAAGGTAAAG	49
99	36[166]	49[160]	AGCGAGAGGCTTTTAAAATGTTGATAACTGGAGC	34
100	64[233]	23[235]	TCAATAGATATACTGGTAATAA	22
101	28[189]	57[181]	CATCGGACCCAAATCAGCAAGGTGTTGGGCCATTCG	36
102	47[203]	44[196]	ATTCTTATAACAACAAAATGATTACCAACGCTAACTGAAGCCCTGTCTT	49
103	65[196]	24[203]	GATTATTTACATTGTTAGAAGGCTTTTGCCACCCT	35
104	38[212]	32[214]	TGATAAGAAAGGAAACCAAACGTAAAGAAACATGGTTTCCG	41
105	47[112]	42[119]	ATTCAAAAGGGTGAGGCAAGGTGGTTTGCTTATAA	35
106	65[49]	24[56]	GATTAGTAATAACAGGCCACCTTGCAGGTCCATTA	35
107	55[161]	34[161]	CGTAACCTTCTCCGAATACCAGGAATTA	28
108	30[149]	23[150]	CTTGAAACACCAGTGAACATCAAGCCAGGCGAAATCCGAGGTTGAAGCC	49
109	40[161]	43[167]	AGAAGCAAATATTATAAGAGAACAACATGTTCAGCTACCAAGTGCGTTTT	50
110	40[202]	43[209]	GGGAGAAAACGTCAGCCAACATAGATAAGTCCTGATAATCGGTTAAATC	49
111	22[62]	63[55]	TGATACCGATAGTTCTGAGGCGAGTAAAAGTGTAG AACAACAACAACAACAACAACAAC	59
112	34[189]	52[175]	GTTTATATACATAACCATGATTGGATTCG	29
113	1[215]	44[217]	GGAACCCCATTTTATCGTTGCTATAGAAAC	30
114	59[203]	30[203]	GAATATACTTTGAACCATCGAATTAGAG	28
115	47[26]	40[42]	TTTTTTTTAGAAGCCTTTATTTCAGTAATACGAGTCAAAGGGCGACAGGATT	52
116	52[233]	7[233]	AATAGTGAATCATACATCAAAGTTGGAATAGGTG	34
117	61[140]	28[138]	CTCTAGACCAAGCTTGACCTTTAAGGCTTG	30
118	19[215]	61[220]	AATGAATCACACCCTCTCAGAGCTTCCTGATCTG	34
119	14[233]	14[215]	GAGGCTGAGACTGATCTAA	19
120	57[203]	54[197]	GGCGAATAACAAAAAAATTATAGGGAGGGAAGGTAAATAGAATTTCCC	48
121	63[221]	69[241]	ACCTGGCCAACAGAGATAGATCTAAAATAGATGTA	35
122	50[241]	5[241]	TACATCAAAGAACGCGAGAGATAGCAATAAGAGTTTAGTACCGCGATGTA	50
123	51[161]	38[161]	ACGTTAAACCCCGGTTTAGACCAAATGC	28
124	80[241]	51[241]	TACATCGCAGCAAATGAACAATCGCAAGACGATGTA	36
125	53[201]	50[197]	CATAGCGATGGTCTGATGTTAGCGAGGAAACGCAATAACCGAAGTAGTTA	50
126	27[138]	30[138]	GCTGCATGCAGGGGGATGTGCTGATTACGCCTGACGATAATCATTG	46
127	47[91]	42[98]	CTGAGTAATGTGTAAATTAAGGTTGCAGCCGAGAT	35
128	63[98]	22[104]	CGCCGCTTGAGTGAGAAACAAAGTACAACAACGGCAAAGACAATTGTATC	50
129	91[49]	90[49]	TTTTTGGGGTCGAGGTGCCGTAGAGGCGGTTTGCGTATTGGG	42

130	65[158]	24[161]	GGAAATACCTAAATCCTGCGCAGTCCAGCAT	31
131	62[111]	65[115]	TGCCTAAACAGGGCGACAGGAGTAATATCCAG	32
132	5[215]	47[220]	CGTCACCAGGCAAGAAAATTGAGAATAAGAAAAG	34
133	57[161]	32[161]	AACCAGGGACGACAGAACTGGACTAACG	28
134	16[241]	16[215]	TACATCACCTATTATTCTGATCGTCTT	27
135	66[235]	67[233]	TAATAGAGACCAGTAATAAAAGGGACATCACTAACA	36
136	24[231]	19[234]	AGAACCGCGTGCCCGTATA	19
137	55[203]	34[203]	ACAGTACAATTAATAATTCATGCAAAGA	28
138	49[200]	40[203]	CTAAATTTAACCGGAATAGATAACATTAGAC	31
139	24[126]	62[112]	TTGATACGAGGGTAGCGGAGATCCTGGGG	29
140	55[174]	32[185]	CTGCCATTGAATTACAGCGAGTAGTTTGTCACAATCAAAAGAAAAAT	47
141	54[233]	9[233]	TTGCTTCTGTCCAAAGAGTGGCAAGTCGAGAGGG	34
142	22[184]	63[181]	ACTAAAGGAATTTACCGCGACAACTTTTAAA	31
143	61[131]	65[139]	GCCATAAAGCTTTGACAGGCCGACCGCCAGCCATTGC	37
144	43[210]	38[213]	AAGATTACTGAATCAAATAGCGAAGCGCCCACAAGACAA	39
145	37[188]	34[190]	GGAATCTTATAACGGCTTATTAGAATAA	28
146	15[215]	57[220]	AGTTTTGAAAGTTTGCACCGTAAGATTCGCTTCA	34
147	58[196]	61[202]	GTTACACTGTTTAACATAAAGAGCATAATCCTGATT	36
148	45[56]	42[57]	ATTTGGGGAGTAGAGTAGCTCAACATGTAAGAGTCCACTAT	41
149	60[233]	15[233]	AACCTACCATTTCATAAAGAATCACATGAAAGTA	34
150	44[233]	43[231]	TACGAGCATGTTTTGCAC	18
151	76[233]	55[233]	AATATCAAGGGTGAGTGAAT	20
152	33[138]	36[138]	AGCCGTAATCCATCAAAAATAATTTTTAACCATAACCGAAGTTTTG	46
153	54[196]	57[202]	TTAGAATGCTTTTTTCATTTAAGGAAATCGCGCAGA	36
154	65[70]	24[77]	CCTGAGTAGAAGAAAAGTGTTTTTTGCGAGACTTT	35
155	61[203]	58[197]	GTTTGGACACGTAACTTATTAGTCAGACTGTAGCGAATGAAATACCAA	48
156	44[153]	50[150]	TCATCGACAATAAATATAAAGTCACCATTATTTTTTGAGAGTTCAG	46
157	78[233]	53[233]	CATCACCTCGCGCTGAGAAG	20
158	47[69]	42[77]	TCATATATTTTAAATAGCATAATCACCGCTTCCAGT	36
159	13[215]	55[220]	GCGTAACCCTGAGCCAAGGTGAAACAAACAAATA	34
160	32[184]	53[181]	CTACGTTAATCTAATGCAACAACCTCATCAA	31
161	91[70]	90[70]	\biotin\ AAAGCACTAAATCGGAACCCTTGAATCGGCCAACGCGCGGGG	42
162	24[160]	61[160]	TGACAGGCGACCTGCAATTCCCGGGTAC	28
163	34[160]	51[160]	CGAGGCAACCAGACTAAATCAATTGTAA	28
164	10[233]	10[215]	GGCGGATAAGTGCACAGAC	19
165	43[84]	40[77]	TAAAGTAAGTGTTGCTGGCCCGAGCTTCAAAGCGA	35
166	44[69]	47[68]	TGCGAACGCGCGAGTCGGTTGGAACCCAACAACAACAACAACAACAACAAC	51
167	42[56]	44[49]	TAAAGAACTAATGCTTTTAGTT	22
168	63[119]	24[127]	ATGGTTGTGTAAAGTTGTATCATCGCCTTTGGCC	34
169	48[233]	3[233]	TAAGGCGTTATTAAGCCAACATAAACCCTCAGAA	34
170	63[56]	22[63]	CGGTCACGACGGGGCTAAAACACTCATCGGAAGTTGAGTTAAAACAGCT	49

171	7[215]	49[220]	ACTACAACCACCAGAAAGTAAGCAAAACTTAAAT	34
172	22[235]	63[220]	GTTTTAAAACAACTTTCAAAGGAGTGATACATTAACC	37
173	90[91]	91[91]	AAAGGGAGCCCCCGATTTAGAGCTTAAACCTGTCGTGCCAGCTGCATTAA	50
174	84[233]	47[233]	TATTAACACAACGCTCAACA	20
175	72[233]	59[233]	CAACAGTTGCTTTACATCGG	20
176	65[179]	24[182]	CTCAATCGTCAACAATTTTCCAGTGAACCAC	31
177	57[221]	75[233]	ATTGACAATATTTTTGAATACCCTCAA	27
178	58[233]	13[233]	AACAATAACGTCAGTAGACCGACTTCAAGAGAAG	34
179	0[233]	0[215]	AGGGATAGCAAGCCCAATA	19
180	9[215]	51[220]	AGCATTCCCCATATAAGAAAATATTATCAAGCAA	34
181	40[76]	43[83]	AAAAAAAAAAAAAAAAAAAAAAAAACCAGACTTGCCCTAGC TAAACTGAAAAGGTGGCATTGATTCATGCAAC	73
182	63[203]	22[210]	TTGCGGAATGATGGTAGAACCGCCTCCCAGAGCCAATGATACCAGTTTC	49
183	30[202]	55[202]	CCAGCAATTGACGGTTAATTAAATGGAA	28
184	4[241]	4[215]	TACATCCACCCTCAGAACCGTGAGTTT	27
185	65[217]	65[235]	CACCAGTCACACTTAGAGC	19
186	23[17]	25[41]	TTTTTTTTCCACGCATAACCACGCAAAGCGGGCGCTA GGGCGGGAAGACGAAAGA	55
187	43[168]	40[162]	AGCGAACTTTGCCAAATCCAAAGCTATTATAGTC	34
188	31[138]	34[138]	TGCACTCCATAGGTCACGTTGGTGGATTGAATTCATCAGCAACACT	46
189	74[233]	57[233]	TATCTGGTCAACCTGAGCAA	20
190	50[149]	57[150]	AAATATTTAAGCTCATTTCGCGTCAAACGGCGTAGATGCCTCAGGCTTC	49
191	24[97]	65[90]	GCTTTGACAAGCGCGCTAACTCACATTACGCCGCGTCCTGAGCTCAAAC	49
192	38[182]	51[173]	TCATTGAAAGAGGGTGTGATAAATTAATGAGAATCGCATATGTTATTTT	49
193	24[76]	62[70]	AAAAAAAAAAAAAAAAAAAAAAAATTCATGATTTGACCTGCGCTC	45
194	62[241]	17[233]	TACATCATTATCATCATACGCCACCAATCACCGCCTATTTCGGAGATGTA	49
195	52[174]	55[173]	CATTAAACCAGCTTCGTCGGAGTGCAT	27
196	17[215]	59[220]	TCCAGACCTGGAACCACCATCTTATCAAAAAGTA	34
197	47[174]	42[182]	CTAGCTTTAGTATCATAGGCAGACGATTTTTTCCAG	36
198	22[167]	65[157]	TAATAATTTTTTCAATGGAAATTTAGAATCAGAGCAAAACGCTCAT	46
199	24[181]	27[189]	CACCAGAGCCGGAATGTGAAATAATCATGGTCATAAATTGCGTTCATTTT	50
200	53[221]	79[233]	AGACGAACTGATAGCCCTAAAAAATCT	27
201	62[69]	65[69]	AGTCGGGGCTGCGCTCAGTGATCACTTG	28

24. The caDNAno design of the DNA origami nanofork

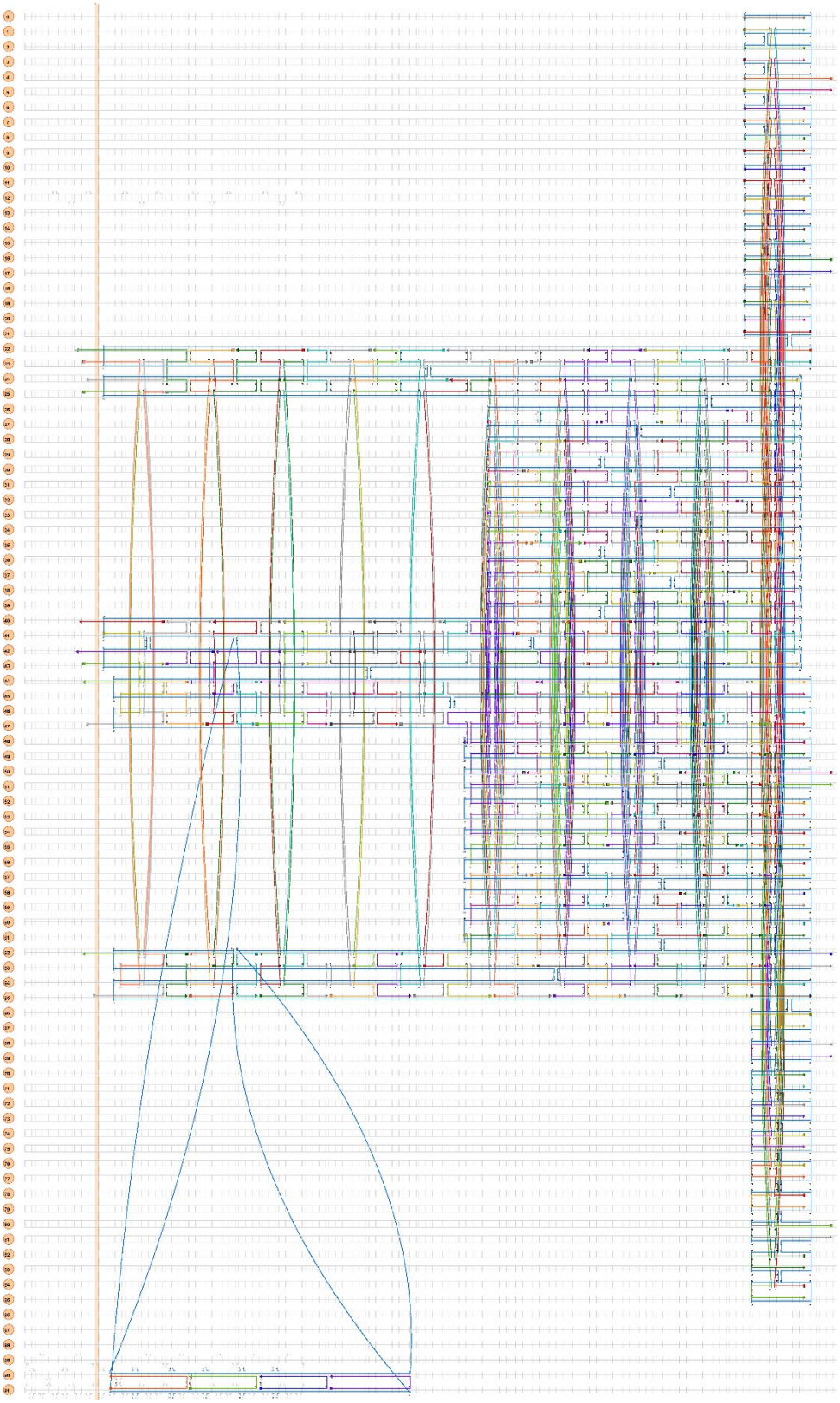

Figure S39. the caDNAno design of the DNA origami nanofork.

25. References

(1) Jaworska, A.; Pyrak, E.; Kudelski, A. Comparison of the Efficiency of Generation of Raman Radiation by Various Raman Reporters Connected *via* DNA Linkers to Different Plasmonic Nano-Structures. *Vib. Spectrosc.* **2019**, *101*, 34–39. DOI: 10.1016/j.vibspec.2019.01.002.

(2) Salmon, A. R.; Kleemann, M.-E.; Huang, J.; Deacon, W. M.; Carnegie, C.; Kamp, M.; Nijs, B. de; Demetriadou, A.; Baumberg, J. J. Light-Induced Coalescence of Plasmonic Dimers and Clusters. *ACS Nano* **2020***, 14* (4), 4982–4987. DOI: 10.1021/acsnano.0c01213.

(3) Johnson, P. B.; Christy, R. W. Optical Constants of the Noble Metals. *Phys. Rev. B* **1972**, *6* (12), 4370–4379. DOI: 10.1103/PhysRevB.6.4370.

(4) Thacker, V. V.; Herrmann, L. O.; Sigle, D. O.; Zhang, T.; Liedl, T.; Baumberg, J. J.; Keyser, U. F. DNA Origami Based Assembly of Gold Nanoparticle Dimers for Surface-Enhanced Raman Scattering. *Nat. Commun.* **2014**, *5*, 3448. DOI: 10.1038/ncomms4448.

(5) Pierce, D. T.; Spicer, W. E. Electronic Structure of Amorphous Si from Photoemission and Optical Studies. *Phys. Rev. B* **1972**, *5* (8), 3017–3029. DOI: 10.1103/PhysRevB.5.3017.